FULL PAPER

Mapping the Stereochemistry and Symmetry of Tetracoordinate Transition-Metal Complexes

Jordi Cirera,[a] Pere Alemany,[b] and Santiago Alvarez*[a]

Abstract: A continuous shape and symmetry study of tetracoordinate transition-metal complexes is presented, in an attempt to provide a systematic description of the stereochemistry of the metal coordination sphere in this important family of compounds. A tetrahedron/square-planar symmetry map has been developed, the main distortion paths of the ideal geometries are presented, and the applicability of a sawhorse shape measure is discussed. More than 13,000 structural data sets have been analyzed and the corresponding stereochemistries assigned from the values of their tetrahedral and square-planar symmetry measures. A good number of structures that are quite distant from the two ideal geometries can be adequately described as snapshots along the spread pathway for their interconversion, making use of the corresponding path deviation function. Further analysis of the structural data by metal electron configuration or by the denticity and conformation of the ligands provide general rules to describe the stereochemical preferences of tetracoordinate transition metal centers.

Keywords: continuous symmetry measures · coordination modes · symmetry maps · tetracoordination · transition metals

Introduction

Tetracoordination is widespread throughout the transition-metal series and a good knowledge of the stereochemical preferences of compounds based on tetracoordinate transition-metal centers is a must for controlling their architecture and properties. The two ideal structures for tetracoordinate complexes are the tetrahedron (T_d symmetry), and the square (D_{4h} symmetry), and a few general rules allow us to classify tetracoordinate molecules in one of these two geometries for certain electron configurations (not to forget the less common sawhorse or octahedral *cis*-divacant geometry). Thus, there is general agreement that metal ions with a d^8 electron configuration prefer the square-planar geometry, whereas d^0 and d^{10} ions are essentially tetrahedral,[1] and that tetrahedral geometry is favored for small metals and large ligands.[2] Less universally accepted trends proposed include the tetrahedral nature of d^4 or high-spin d^5 complexes.[1]

Besides, it is not always possible to adequately describe a tetracoordinate molecular structure with one of the above-mentioned ideal shapes. Thus, in many cases intermediate structures can be found, or the same molecule may even appear in different coordination environments in different crystal structures or in different crystallographic positions of the same crystal structure. As an example, Keinan and Avnir[3] recently showed that the structures of the $[CuX_4]^{2-}$ (X = Cl, Br), $[NiX_4]^{2-}$ (X = Cl, CN) and $[PtX_4]^{2-}$ (X = Cl, Br, I) ions all fall along the path that interconverts the tetrahedron and the square. Similar deviations from ideality can be found for other metal ions affected by the presence of bidentate ligands.[4] Given the close relationship between chemical reactivity, physical properties, and molecular structure, there is a need for a more accurate, yet simple, description of the geometry of the coordination sphere of a transition-metal atom than the rather crude assignment of one of the ideal shapes (tetrahedron, square, or sawhorse).

Theoretical studies aimed at rationalizing the stereochemistry of tetracoordinate complexes have faced similar problems. Thus, a qualitative molecular orbital analysis[5] suggested that the situation for electron configurations other than d^0, d^8 and d^{10} is not so simple and significantly distorted structures

[a] J. Cirera, Prof. S. Alvarez
Departament de Química Inorgànica
and Centre de Recerca en Química Teòrica
Universitat de Barcelona, Diagonal 647
08028 Barcelona (Spain)
Fax: (+34) 93-4907725
E-mail: santiago.alvarez@qi.ub.es

[b] Dr. P. Alemany
Departament de Química Física
and Centre de Recerca en Química Teòrica
Universitat de Barcelona, Diagonal 647
08028 Barcelona (Spain)
E-mail: santiago.alvarez@qi.ub.es

should be expected. Burdett provided structural predictions for all d^n electron configurations[6] based on the Jahn–Teller instability of the tetrahedral geometry for each configuration, but no systematic comparison with experimental structural data was confronted with those predictions. Also a molecular orbital rationale for the stereochemical preferences of d^0, d^8 and d^{10} ions has been given by Albright, Burdett and Whangbo.[7]

The proposal of Avnir and co-workers to define molecular symmetry or shape as continuous structural properties[8, 9] has caught our attention, and some effort has been devoted by us in recent years to explore the applicability of the *continuous symmetry measures* (or continuous shape measures) to the analysis of structural correlations and structure–properties correlations.[10–12] According to Avnir, rather than describing a molecular structure as having a certain symmetry or not, it is most useful to use a quantitative measure that tells us how far (or how close) that structure is from a specific symmetry or shape. Therefore, a continuous symmetry measure (abbreviated from here on as CSM) for a molecular structure is defined as the distance to an ideal symmetry, independent of size and orientation. Similarly a continuous shape measure calibrates the distance to a chosen reference shape.

In some cases, shape and symmetry measures are equivalent. This is the case of the tetrahedron, for every tetrahedron has the full T_d symmetry. Conversely, every tetracoordinate center with T_d symmetry must have four identical bond lengths and four identical bond angles. In other cases, shape is a more stringent criterion than symmetry, as in a trigonal bipyramid,[11] for which we have adopted a reference shape with all bond lengths identical, while an infinite number of trigonal bipyramids with D_{3h} symmetry exists, differing from each other in the ratio between axial and equatorial bond lengths. Therefore, all trigonal bipyramids with bond length ratios larger or smaller than one (our choice of reference shape) will have finite values for the shape measures, even if

Abstract in Spanish: *En este artículo se presenta un estudio de forma y simetría continuas sobre complejos tetracoordinados de metales de transición, en un intento de proporcionar una descripción sistemática de la estereoquímica de las esferas de coordinación de los metales en esta importante familia de compuestos químicos. Se desarrolla un mapa de simetría referido al tetraedro y al cuadrado, se presentan los principales caminos de distorsión de estas geometrías ideales y se discute la aplicabilidad de la medida de forma de caballete. Se han analizado más de 13 000 conjuntos de datos estructurales y las correspondientes estereoquímicas se han asignado a partir de los valores de sus medidas de simetría tetraédricas y plano-cuadradas. Un número significativo de estructuras que aparecen distantes de ambas geometrías ideales se pueden describir razonablemente como instantáneas a lo largo del camino de interconversión, haciendo uso de la correspondiente función de desviación del camino. Un análisis detallado de los datos estructurales clasificados según la configuración electrónica del metal o según la denticidad y conformación de los ligandos nos ofrece unas reglas generales para describir las preferencias estereoquímicas de centros metálicos tetracoordinados.*

they have the full D_{3h} symmetry. In the present work we will in general refer to shape measures, even if those relative to the tetrahedron and the square could be correctly termed symmetry measures.

In the work reported here we have studied in a systematic way the experimental structures of a representative sample of tetracoordinated transition-metal atoms by using their symmetry measures relative to the tetrahedron, $S(T_d)$, and to the square, $S(D_{4h})$. To that end we will carefully analyze the mapping of the different distortions of these two reference structures in the space of these two symmetry measures by using a molecular ML_4 model that includes only the metal and donor atoms. We will show how the particular distortion presented by a specific molecule can be in most cases easily identified by representing its T_d and D_{4h} symmetry measures in a two dimensional scatterplot (a *symmetry map*). With such map in hand, we will then explore the experimental behavior of tetracoordinate complexes as a function of the metal electron configuration and as a function of the constraints imposed by some bi- or multidentate ligands, in search for general rules about their stereochemistry.

Results and Discussion

Continuous shape and symmetry measures—methodology: For molecules or molecular fragments that can be approximately described by a polyhedron (eventually including a central atom, as in coordination compounds), the coordinates of the N atoms are given by the vectors $\vec{\mathbf{Q}}_k$ ($k = 1, 2, .., N$), whereas the coordinates for the perfect polyhedron closest in size and orientation are given by the vectors $\vec{\mathbf{P}}_k$ ($k = 1, 2, .., N$). The *distance* of the molecular structure to the perfect polyhedron belonging to a symmetry point group G is then defined as Equation (1):[13]

$$S(G) = \frac{\sum_{k=1}^{N} |\vec{\mathbf{Q}}_k - \vec{\mathbf{P}}_k|^2}{\sum_{k=1}^{N} |\vec{\mathbf{Q}}_k - \vec{\mathbf{Q}}_0|^2} \times 100 \tag{1}$$

in which $\vec{\mathbf{Q}}_0$ is the coordinate vector of the geometrical center of the investigated structure. With such definitions, it has been shown that the bounds for any symmetry measure are $0 \leq S(G) \leq 100$. The lower limit corresponds to structures that exactly match the shape of symmetry G, and increasing values result for increasingly distorted structures. A very useful property of the symmetry measures is that they allow us to compare on the same scale the proximity of different molecules to the same symmetry, or of the same molecule to different symmetries. One can also calibrate on the same scale different distortions from a particular ideal structure.

Symmetry maps for tetracoordinate complexes: In previous work, we have found that a convenient way to analyze molecular structures of a given coordination number is to generate a scatterplot of the symmetry measures relative to two characteristic polyhedra with the same number of vertices.[10, 12] In such symmetry maps, each coordination geometry occupies specific regions and distortion pathways

are represented by well-defined lines. As a consequence, the position of a given molecular structure in the symmetry map provides us with an approximate description of the polyhedron that best describes its coordination sphere, as well as of the type and degree of distortion from such a polyhedron. For the case of tetracoordinate atoms, we will consider one basic symmetry map corresponding to the interconversion of the tetrahedron and the square.

The geometrical T_d–D_{4h} map: Focusing on the tetrahedon–square symmetry map, we wish first to determine which regions of the symmetry map are geometrically possible. To that end, we have randomly generated five million ML_4 structures with the only constraint that the four M–L distances are identical and have calculated their symmetry measures relative to both the tetrahedron and the square. The results are plotted in Figure 1, in which the geometrically
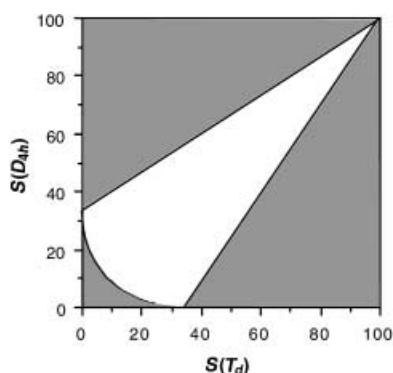

Figure 1. Geometrically allowed region of the symmetry map for tetracoordination (white area). A set of 5×10^6 randomly generated ML_4 structures were all found within that region.

inhabitable region of the symmetry map appears as a wedge-shaped island. The sea around that island corresponds to combinations of the two symmetry measures that are geometrically impossible and a little thought allows us to understand the shape of that island:

1) The (0,0) point is by definition unreachable, since it would correspond to a structure that has at the same time perfect tetrahedral and square-planar symmetries.

2) There is only one allowed point at each coordinate axis, because the distance from a perfect polyhedron (i.e., a zero value for one symmetry measure) to the alternative one (i.e., the second symmetry measure) has a unique value.

3) The case in which all the vertices of a polyhedron have collapsed to a single point has, by definition [Eq. (1)] a symmetry measure of 100 relative to any ideal polyhedron, hence the only allowed point with $S(T_d) = 100$ is the one with $S(D_{4h}) = 100$ and vice versa.

An experimental T_d–D_{4h} symmetry map: Next we look at all geometries of tetracoordinated transition-metal atoms, as retrieved from molecular structures in the Cambridge Structural Database (see Appendix for criteria applied to database searches), to which a less comprehensive data set of inorganic solids from the ICSD database was added. A total of 13 417

crystallographicaly independent data sets were found, and the calculated symmetry measures are presented in Figure 2. It can be seen there that, among all the geometrical possibilities seen in Figure 1, only the lowermost portion is actually inhabited by real molecules. The region of high-symmetry measures is severely inhospitable for reasons that will be seen below.
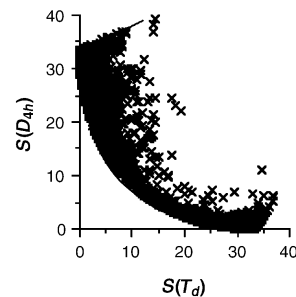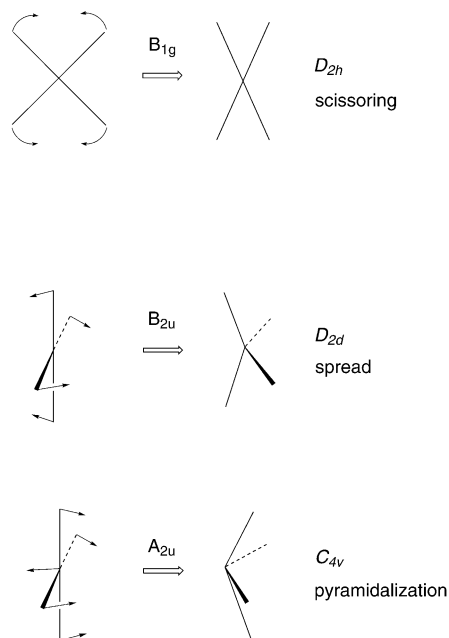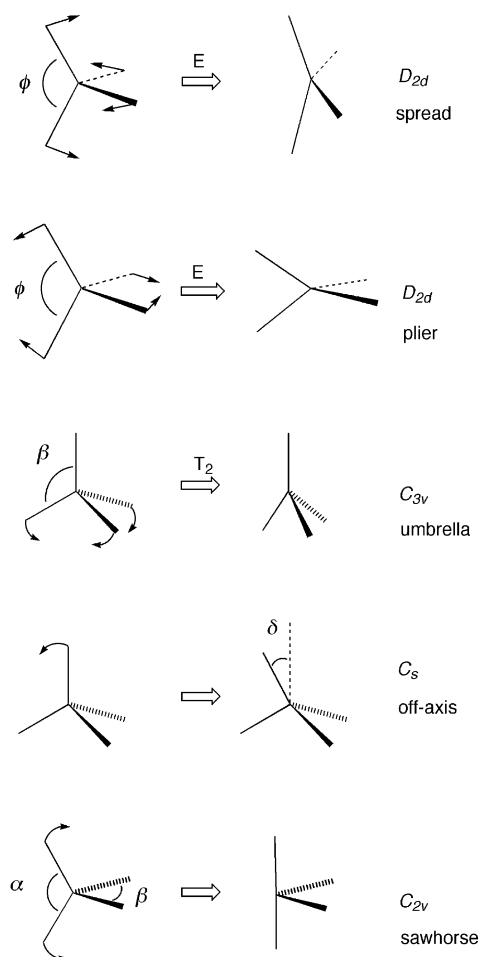

Figure 2. Experimental ML_4 structures from the CSD (13 417 data sets) in the symmetry map for tetracoordination.

Ideal polyhedra and distortion pathways: We turn now to those tetracoordinate geometries that are most likely to be found in real molecules. We thus analyze angular distortions of the tetrahedron and the square, since previous studies[11] indicate that bond length distortions affect the symmetry measures much less than bond angle distortions. The distortions to be analyzed are summarized in Scheme 1 (for the tetrahedron) and Scheme 2 (for the square); here we present the symmetry subgroup of the distorted molecule, the name used in this paper to refer to each distortion mode, and a graphical depiction of the corresponding distortion mode together with a symmetry label for those distortion coordinates that are symmetry-adapted.

Scatterplots of the square planar and tetrahedral symmetry measures for some of these distortions are presented in Figure 3 (top), as calculated for an MX_4 molecular model. For the time being we introduce no chemical restrictions on the angular distortions, which in some cases are taken to unrealistic extremes. For example, the umbrella distortion is taken to the extreme at which three X atoms are superimposed. Although such extreme distortions are meaningless from the chemical point of view, they will prove highly helpful for understanding the relationships between different distortions and their positions in the symmetry map.

The first observation that can be made is that three distortion paths mark the borders of the uninhabited land in the map, a wedge comprised between the three points (0, 33.3), (33.3, 0), and (100, 100). This result is consistent with the distribution of the random structures in Figure 1, and limits the inhabitable region of the symmetry map to the wedge-shaped island. A second characteristic that can be detected is that there are three limiting points (labeled a–c in Figure 3, top). Point a corresponds to the collapse of the four vertices (i.e., the four donor atoms in a coordination complex) onto the same position in space; this can be achieved either by pyramidalization (C_{4v}, Scheme 2) or umbrella-closing distortion (opposite to the C_{3v} umbrella-opening distortion depicted

© 2004 Wiley-VCH Verlag GmbH & Co. KGaA, Weinheim **www.chemeurj.org**
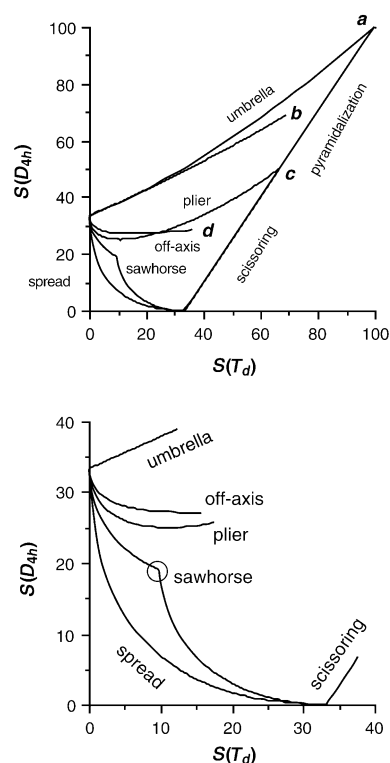
Scheme 1.

Scheme 2.

Figure 3. Symmetry map for geometrical distortions of the tetrahedron and the square (see Schemes 1 and 2) showing the distortion paths taken to the extreme at which some atoms collapse (above), and blow-up of the chemically significant area of the symmetry map (below). The circle indicates the position of the reference sawhorse adopted in this work.

in Scheme 1). Point b corresponds to the collapse of three vertices at the position opposite to the fourth one, resulting from the umbrella-opening distortion (as under a strong wind)

of C_{3v} symmetry (Scheme 1). Finally, point c results when the four vertices are grouped in pairs in a linear arrangement with the central atom, as results from the extreme plier and scissoring distortions of the tetrahedron and the square (see Schemes 1 and 2, respectively). The scissoring distortion coincides with part of the pyramidalization path in the symmetry map, but the former ends at point c, whereas the latter goes all the way to point a. It is worth analyzing in more detail these two last distortions. The scissoring distortion represented in Scheme 2 and its inverse are equivalent and are represented by a single line in the symmetry map. In contrast, the plier distortion represented in Scheme 1 goes directly to the 2+2 collapse point c, whereas its opposite is the spread path that converts the tetrahedron into the square planar form continuing from there [the (33.3, 0) point] to the same point c. The presence of collapse points in the region of high CSM values explains why this region of the island is "inhospitable" to chemical entities, in agreement with it being unpopulated in Figure 2. Hence, we will restrict ourselves from here on to the study of the region of the symmetry map with CSM values of at most 40 units (Figure 3, bottom). For brevity, we will not discuss here the dependence of the symmetry measures on the angular parameters for the different distortions, but the reader may find the corresponding plots as Supporting Information.

Let us now take a closer look at the distortion lines in the symmetry map. We start by discussing the spread/planarization pathway, which has been in part analyzed in previous

papers.[3, 14] The perfect tetrahedron is characterized by $S(T_d) = 0.00$ and $S(D_{4h}) = 33.33$. Conversely, the perfect square is characterized by $S(D_{4h}) = 0.00$ and $S(T_d) = 33.33$. The symmetry measures of any molecular structure Q along the minimum distortion path that connects the tetrahedron and the square must obey Equation (2),[14] in which $\theta(T_d, D_{4h})$ is a characteristic constant of that path and is related to the symmetry measure of one polyhedron relative to the other, as indicated in Equation (3).

$$\arcsin\frac{\sqrt{S_Q(T_d)}}{10} + \arcsin\frac{\sqrt{S_Q(D_{4h})}}{10} = \theta(T_d, D_{4h}) \tag{2}$$

$$\sin\theta(T_d, D_{4h}) = \sqrt{\frac{S_{T_d}(D_{4h})}{100}} = \sqrt{\frac{S_{D_{4h}}(T_d)}{100}} \tag{3}$$

Our model spread route may also be fitted to an exponential[3] or to a square root sum [Eq. (4)], but the expression in Equation (2) provides a better agreement and has been shown to correspond to the minimum distortion path. Similar expressions apply for the minimum distortion path between every pair of polyhedra of an arbitrary number of vertices, and the minimum distance constants $\theta(A, B)$ have been given elsewhere.[14]

$$\sqrt{S(T_d)} + \sqrt{S(D_{4h})} = 5.77 \tag{4}$$

If the deviation of a given molecular structure from an ideal symmetry can be quantified by the corresponding symmetry measure, its deviation from the interconversion path between two ideal structures be evaluated by the deviation function[14] defined in Equation (5), for which $\theta(T_d, D_{4h})$ is defined in Equation (3).

$$\Delta(T_d, D_{4h}) = \left| \arcsin\frac{\sqrt{S_Q(T_d)}}{10} + \arcsin\frac{\sqrt{S_Q(D_{4h})}}{10} - \theta(T_d, D_{4h}) \right| \tag{5}$$

As expected, any distortion of the tetrahedron results in an increase of $S(T_d)$, indicative of a decreased tetrahedricity. But, quite interestingly, each distortion behaves differently with respect to square planarity. In three cases the distortion of the tetrahedron is accompanied by different degrees of approximation to a square, indicated by a decrease in the values of $S(D_{4h})$. In contrast, the umbrella distortion takes the molecule away from the tetrahedron and also further away from the square. Note that, within the chemically meaningful region, the symmetry measures follow the same path for an increase than for a decrease in the bond angle β from the tetrahedral value (i.e., opening and closing the umbrella have the same effect on the symmetry measures). Except for the region in which the spread and umbrella distortions show similar pairs of CSM values, in general, the position of a particular structure in the two-dimensional space allows one to easily identify the distortion that is present. The opposite of the umbrella distortion, the Walden inversion, has also been studied previously from the standpoint of the continuous symmetry measures.[15] An interesting observation is that a sawhorse structure with $\alpha = 180°$ and $\beta = 109.47°$ (Scheme 1) is isosymmetric relative to the tetrahedron and the square, with $S(T_d) = S(D_{4h}) = 11.62$. If instead we consider a sawhorse that corresponds to the cis-divacant octahedron ($\alpha = 180°$,

$\beta = 90°$), it is closer to the tetrahedron, $S(T_d) = 9.8$, than to the square, $S(D_{4h}) = 19.1$ (encircled in Figure 3, below)

The sawhorse as a reference shape: Even if the sawhorse geometry **1** is not a very common one, it bears wide interest because of 1) the possibility of carrying out association reactions on the open side of the metal atom, 2) the ability of some such structures to form agostic interactions with pending groups of coordinated ligands,[16] and 3) the possibility of fluxional behavior through an intermediate square-planar geometry.[17] Geometrically, a sawhorse is characterized by a large bond angle (maybe close to $180°$) between the two transoid ligands and a small angle (of around $90°$) between the two cisoid ligands. From a symmetry point of view, the sawhorse belongs to the C_{2v} point group, actually a subgroup of both T_d and D_{4h}. All this means that the sawhorse is neither distinct from the tetrahedron or the square in terms of symmetry nor is it univocally defined, there being a wide choice of combinations of transoid and cisoid bond angles (α and β in **1**) that could correspond to C_{2v} sawhorses.

We can consider three reasonable geometries to define an ideal sawhorse: 1) a cis-divacant octahedron, 2) a trigonal bipyramid with a vacant equatorial coordination site, and 3) an intermediate structure in the asynchronous transformation of a tetrahedron into a square (in contrast with the spread pathway in which the transformation is synchronous). Even if we arbitrarily choose the reference sawhorse to have a bond angle of $180°$ between transoid ligands, the angle between cisoid ligands would be 90, 120, or $109.47°$ for each of the three choices outlined. An additional geometrical restriction imposed by the C_{2v} symmetry is that the angle between the corresponding ML_2 planes must be $90°$. In spite of the wide variability of the cisoid angle, we can view such structures as distinctly different from both the tetrahedron and the square, and will not be surprised that the molecular structures of compounds such as $[RuH_4]^{4-}$ (Figure 4) or compounds with
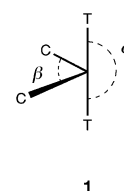

1

Figure 4. Coordination sphere of some complexes (Table 2) that can be classified as sawhorse structures, from left to right: $[RuCl_2(PPh_2Xyl)_2]$, $[RuH_4]^{4-}$, $[V(tmen)(OPh\{Ph\}_2)_2]$ and $[Cu(scyclam)]^+$ (see Table 2 for references).

more elaborate ligands and a variety of metal electron configurations (Table 1) are described as sawhorses, but not as distorted tetrahedra or squares. In this work we will consider the ideal sawhorse to correspond to a cis-divacant octahedron (i.e., $\alpha = 180°$, $\beta = 90°$), and the sawhorse shape measures, S(sawhorse), are thus measured with reference to that specific choice.

Table 1. Distribution of molecular structures analyzed according to electron configuration and assignment to tetrahedral, square planar, intermediate (spread) or sawhorse geometries, according to the corresponding symmetry measures.

d^n	Total	CSD	ICSD	T_d	D_{4h}	spread	sawhorse	unassign.	metals
0	526	474	52	513	2	1	3	7	Cr, Hf, La, Mn, Mo, Nb, Os, Re, Sc, Ta, Tc, Ti, V, W, Y, Zr
1	57	49	8	57	0	0	0	0	Cr, Mn, Mo, Nb, Os, Ru, Ta, Ti, V
2	66	62	4	63	2	0	0	1	Cr, Mo, Nb, Os, Ru, V, W
3	17	15	2	7	7	0	3	0	Cr, Fe, Mo, Nb, Os, Re, V
4	82	76	6	20	56	2	2	2	Cr, Fe, Ir, Mn, Os, Re, Ru
5	297	281	16	280	13	1	1	2	Co, Fe, Ir, Mn
6	168	165	3	100	51	2	6	9	Co, Fe, Ir, Mn, Ni, Os, Pd, Pt, Rh, Ru
7	526	519	7	360	144	9	6	7	Co, Fe, Ir, Ni, Pt, Rh
8	7680	7649	31	139	7486	32	6	17	Ag, Au, Co, Cu,Fe, Ir, Ni, Pd, Pt, Rh, Ru
9	2238	2229	9	157	1788	284	5	4	Ag, Au, Co, Cu, Ni, Pd, Pt
10	1760	1755	5	1367	75	45	56	217	Ag, Au, Cd, Co, Cu, Fe, Hg, Ni, Os, Pd, Pt, Rh, Zn
Total	13417	13274	143	3063	9624	376	88	266	

We could in principle detect the sawhorse shape of a particular structure by its position in the tetrahedron/square symmetry map. However, a look at Figure 3 tells us that the sawhorse line is rather close to the spread pathway, hence it is not clear from the values of $S(T_d)$ and $S(D_{4h})$ alone whether a given structure is close to the sawhorse or corresponds to some other distortion from the spread path. After all, the CSM approach also allows us to measure the deviation of a given molecular structure from an arbitrary shape, such as our conventional sawhorse. To see how useful the sawhorse shape measures might be we have searched for structures of tetracoordinate complexes with transoid bond angle of at least 160°, cisoid bond angle between 80 and 100°, and a torsion angle between the two ML_2 planes in the range $80° < \tau < 90°$. Of the 27 structures found (the most distinctive ones are collected in Table 2), 26 have S(sawhorse) values of less than 3.5 and smaller than $S(T_d)$ and $S(D_{4h})$. The only exception[18] corresponds to an Hg^{II} compound with two long

distances to O atoms (2.66 and 2.72 Å, compared to an atomic radii sum of 2.05 Å); this clearly indicates a severe distortion from the sawhorse toward a linear dicoordinate complex. These results suggest that the sawhorse shape measure adopted here provides a good agreement with the qualitative perception of those structures as being much better described as sawhorses than as tetrahedra or squares.

Now that we have seen that structures which can be described as sawhorses from their angular parameters are well recognized as such by the corresponding shape measure, we may ask whether the shape measures would allow us to identify approximately sawhorse structures which are not recognized from their geometrical parameters. We therefore explore the feasiblity of detecting sawhorse structures from their position in the $S(T_d)$ versus $S(D_{4h})$ symmetry map. To that end we choose all those structures that differ at most in 5.0 units from the values corresponding to the ideal *cis*-divacant octahedron ($S(T_d) = 9.78$ and $S(D_{4h}) = 19.05$). We find now 206 structures, only 28 of which have sawhorse shape measures smaller than 3.5, but only 16 of them coincide with those found using the bond angles criterion.

Finally, within the whole set of tetracoordinate structures analyzed in this work, we have just searched for those that have S(sawhorse) of at most 3.5. We found 88 such structures, which included all those found with the two previous criteria. Even when a more restrictive criterion is used (e.g., S(sawhorse) ≤ 2.5) the number of structures found (42) is still quite large. These results confirm that the sawhorse shape measure as defined here is highly useful for detecting those few structures amongst the plethora of distort-

Table 2. Geometrical parameters and shape and symmetry measures of compounds with sawhorse coordination spheres.

Compound[a]	α	β	$S(T_d)$	$S(D_{4h})$	S(sawh.)	$S(O_h)$[b]	Config.	ref.
[V(tmen)(OPh{Ph}$_2$)$_2$]	173	82	6.82	24.74	0.70		d^3	[41]
[Cr(C$_6$H$_3$Cl$_2$)$_4$]$^-$	143	104	3.30	23.40	2.75	7.66	d^3	[42]
[CrEt(tBu$_3$tpb)]	168	107	8.86	14.62	1.46		$d^{4[c]}$	[43]
[RuCl$_2$(PPh$_2$Xyl)$_2$]	168	102	8.38	16.87	0.31		$d^{6[d]}$	[44]
[Ru(CO)Ph(PMetBu$_2$)$_2$]$^+$	168	94	11.11	20.26	0.99		$d^{6[d]}$	[45]
[Co(mIm)(PhNO$_2$)$_2$]	159	97	4.64	21.94	1.24	0.94	d^7	[46]
[Co(py)$_2$(OPhBr$_3$)$_2$]	149	102	3.03	22.72	2.45	4.41	d^7	[47]
[Co(Et-oxsa)$_2$]	149	112	4.91	18.97	2.60	5.38	d^7	[48]
[Co(iPr-oxsa)$_2$]	148	118	5.04	17.10	2.89	5.87	d^7	[48]
[CoCl$_4$]$^{2-}$	154	108	7.23	18.37	3.42		d^7	[49]
[Co(Me-oxsa)$_2$]	147	112	4.57	20.07	3.00	5.86	d^7	[48]
[RuH$_4$]$^{4-}$	170	84	7.68	23.94	0.47	8.59	d^8	[50]
[Ir(CO)(OCH$_2$CF$_3$)(PCy$_3$)$_2$]	162	97	8.56	19.51	0.57		d^8	[51]
[NiBr(tpcdd)]	156	126	8.08	11.58	2.68		d^8	[52]
[Ni(quin)$_2$]	158	106	6.64	19.59	2.70		d^8	[53]
[Ru(CO)$_2$(PtBu$_2$Me)$_2$]	166	133	14.91	8.40	3.45		d^8	[54, 55]
[Cu(scyclam)]$^+$	171	85	6.94	23.87	0.75		d^{10}	[56]

[a] Cy = cyclohexyl; mIm = 1-methylimidazole; oxsa = (N-(2-(4-alkyl-2-oxazolinyl)phenyl)-p-tolylsulfonamido-N,N′); quin = (8-quinolyl)-*tert*-butyldimethylsilylamido; scyclam = 4,11-dibenzyl-1,4,8,11-tetra-azabicyclo(6.6.2)-hexadecane; tmen = N,N,N′,N′-tetramethyl-ethylenediamine; tpb = tris(pyrazoly)borate; tpcdd = 1,5,9-triethyl-1,5,9-triphospha-cyclododecane. [b] octahedricity measure for those cases with two contacts. [c] High spin. [d] Low spin.

ed tetrahedra and squares. By analyzing that single parameter, S(sawhorse), we obtain the same information that would require three parameters (α, β, and τ) if viewed from a geometrical point of view.

We were surprised to find a good number of Hg[II] compounds among the sawhorse geometries, since we expect tetracoordinated d[10] ions to present tetrahedral structures. Thus, the largest part of sawhorse molecules found in our geometrical search correspond to mercury complexes and, still more striking, a 3.2% of the Hg[II] molecules can be assigned a sawhorse geometry according to their shape measures. A closer look at these purported sawhorse structures[18–35] shows that in all cases the distances of the two cisoid ligands (C positions in **1**) to mercury are significantly longer than the sum of the atomic radii, indicating that these are more appropriately described as dicoordinate linear complexes with two additional contacts. Nevertheless, it is remarkable that the numerical value of the sawhorse shape measure has provided us with a simple means of detecting the inadequate coordination number assignment to mercury for those compounds in the structural database.

Distribution of experimental tetracoordinate structures: To get a qualitative idea of the relative importance of tetracoordination throughout the transition-metal series, we plot in Figure 5 the number of crystallograficaly independent molecules found in our reference data set for each metal. It is clearly seen that an overwhelming majority of the tetracoordinate complexes correspond to metals of Groups 9–12, presumably (see below) to the d[8] and d[10] ions Rh[I], Ni[II], Pd[II], Pt[II], Cu[I], Au[III], and Zn[II]. It must be stressed, however, that structurally characterized tetracoordinate complexes are known for all transition metals.

More interesting would be to have a breakdown of such distribution between tetrahedral and square-planar geometries. Since the geometry choice is determined to a great deal by the electron configuration, we will not discuss in detail the

distribution by metal, although a few interesting results are worth a short comment. By looking at Figure 2 we can see that there are many structures that significantly deviate from the two ideal geometries; hence, to classify the structures as tetrahedral *or* square planar is a rather crude approximation. We adopt the arbitrary criterion in this section that a structure can be classified as approximately tetrahedral (or square planar) if its $S(T_d)$ value (or its $S(D_{4h})$ value) is not larger than 5.0, thus leaving some structures unassigned. With such a criterion, we find that tetrahedral structures can be found for all metals, whereas no square-planar structures are found for Sc, Y, La, Ti, Zr, Hf, Ta, Mo, and Tc, and only between one and three square-planar structures each are found for V, Nb, W, Re, Ru, and Os.

Although the breakdown by central metal atom may give some idea about the general trends, the same metal may show a different stereochemistry depending on its oxidation state and on the geometrical constraints imposed by the ligands. As examples let us discuss the distribution of the abundant Pd, Pt, and Zn complexes (2142, 2456, and 581 crystallograficaly independent molecules retrieved, respectively). In the first two cases, most of the structures can be classified as square planar (99.2 and 99.5%, respectively), as would be expected for the d[8] electron configuration in their +2 oxidation state. The small number of tetrahedral Pd and Pt structures (a total of 11 structures) correspond to zerovalent compounds, in agreement with their d[10] electron configuration (let us remark that in two such cases a +2 oxidation state is assigned in the CSD, but the appropriate oxidation state is undoubtedly zero).

For the Zn complexes, most of the structures (84.2%) are tetrahedral, as expected for the d[10] electron configuration of the Zn[II] ion, but there is a significant 11.0% of square-planar structures. What do those structures have in common? Most of the square planar Zn complexes have porphyrin, phthalocyanin, or related unsaturated macrocyclic ligands. The only exceptions to these rules correspond to tri-[36] or tetradentate[37, 38] ligands whose rigidity seems to forbid adaption to the tetrahedral coordination. A nice example of the constrained geometry imposed on d[10] ions by macrocyclic ligands is provided by the family of Zn[II] and Cd[II] tropocoronands prepared by Doerrer and Lippard.[37] In this family of compounds, as the rigidity of the ligand is relaxed by increasing the size of the aliphatic rings ($m + n$ in **2**), the coordination sphere approaches the tetrahedron and an excellent correlation is found between $m + n$ and $S(D_{4h})$, as shown in Figure 6. These findings clearly show that the geometry of the coordination sphere results from a compromise between the electronic preference for a tetra-
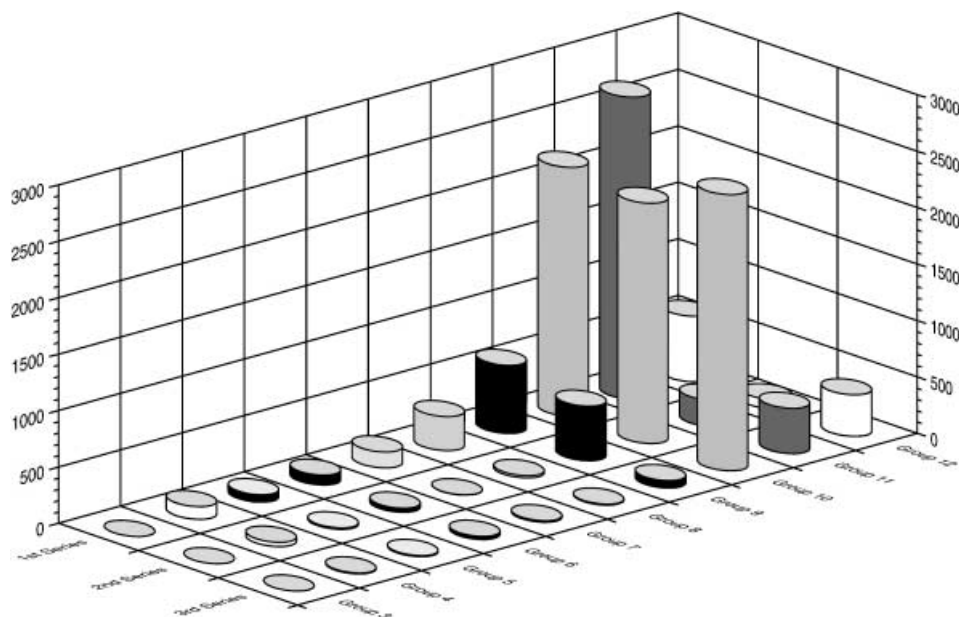

Figure 5. Distribution throughout the transition-metal series of tetracoordinate complexes analyzed in this study.
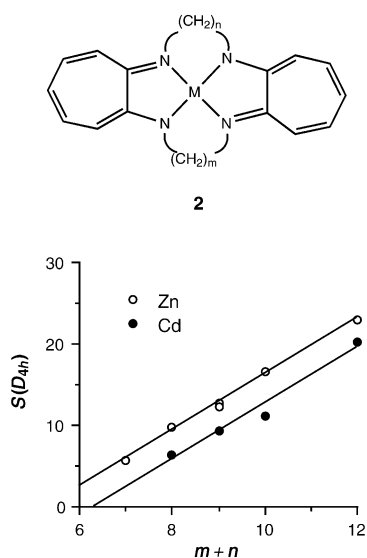
2

Figure 6. Square planarity of Zn^{II} and Cd^{II} tropocoronand complexes as a function of the size of their aliphatic chains.

hedral geometry and the ligand-imposed coplanar arrangement of the donor atoms.

Another special case is that of the copper complexes, for which only an 85.0% of 2667 molecules can be assigned as tetrahedral or square planar within 5.0 CSM units. But the symmetry measures can still help us classify those structures. Taking into account Equation (2), we can analyze the copper structures by adopting the criterion that deviations from the ideal path [Eq. (5)] of 7.0 at most are indicative of geometries close to the spread pathway and are therefore intermediate between tetrahedral and square planar. With such a criterion, 98.2% of the retrieved structures can be classified as tetrahedral, square planar, or in-between. Even if we make the criterion more restrictive by allowing deviations of at most 6.34, still 95.9% of the structures are classified as falling along the spread pathway. In fact, only two complexes present deviations larger than 8.6, and these have multidentate ligands which impose umbrella[39, 40] and inverted umbrella[55] coordination geometries on copper (Figure 7).

Given the influence that the electron configuration and the ligand topology may have on the

Figure 7. Coordination sphere of copper complexes that deviate most from the spread pathway as required by multidentate ligands that force umbrella[40] and inverted umbrella[39] distortions.

stereochemical choice for a given metal atom, we will now analyze the distribution of structures according to electron configuration and then proceed to study in detail how some specific ligands affect the symmetry measures.

Analysis of experimental structures by metal electron configuration: We have analyzed all the structures of tetracoordinate transition-metal atoms retrieved in our structural database search. The results of the continuous symmetry measures for those structures are displayed in Figure 8, grouped
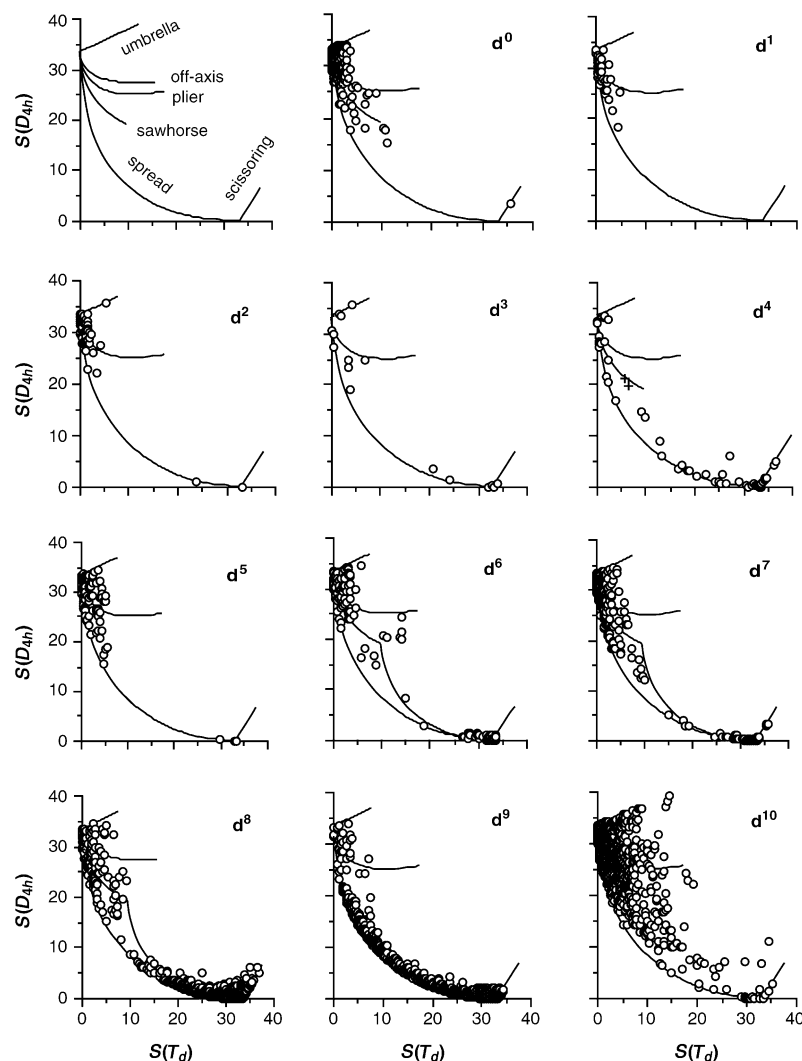

Figure 8. Continuous shape measures of experimental structures for tetracoordinate transition-metal complexes according to their electron configuration. The lines corresponding to different distortions of the ideal geometries are labeled in the first vignette.

according to the electron configuration of the metal atom. The total number of structures for each electron configuration, together with their origin (CSD or ICSD) and the elements found with that configuration are given in Table 1. There we classify the structures as tetrahedral, square planar, or saw-horse according to the smallest of the corresponding shape measures, provided it is smaller or equal than 5.0, 5.0, and 3.5, respectively. In those cases with two shape measures smaller than this threshold, we assign the ideal shape that gives the smaller measure. Among the structures that cannot be clearly identified as tetrahedral or square planar with those criteria, we can assign an intermediate geometry (along the spread pathway) according to the criterion that the deviation function [Eq. (5)] is less or equal than a 15% of $\theta(T_d, D_{4h})$. The number of structures along the spread pathway include the tetrahedral and square-planar ones. The number of structures that cannot be clearly assigned to any of these geometries is indicated as "unassigned" in Table 2.

d^0 ions: One can observe that practically all the d^0 structures cluster around $S(T_d) = 0$ and most of them can be unambiguosly assigned as tetrahedral. The only exceptions correspond to the approximately square-planar $[MO_4]^{2-}$ groups in the extended structures of $SrMO_4$ compounds (M = Mo, W), which may not be strictly considered as tetracoordinate, given the existence of two additional M···O contacts at ~2.5 Å, and possibly also of metal–metal bonding (~2.6 Å).[57]

As for the small distortions from the tetrahedron, most structures are distributed along the spread distortion pathway, as indicated by deviation functions [Eq. (5)] smaller than 15% of the $\theta(T_d, D_{4h})$ constant. Those structures with deviations larger than that value can be classified into three groups.
1) Several structures that have $S(D_{4h})$ values larger than 33.6 correspond to $[MXL_3]$ complexes,[58–64] (M = Ti, Zr, Hf; X = NMe$_2$, NEt$_2$, OtBu, CH$_2t$Bu, SiMe$_3$; L = Si(SiMe$_3$)$_3$ or Ge(SiMe$_3$)$_3$), in which the M−X bond is significantly shorter than the three M − L ones.
2) Three molecules are significantly distorted along the spread pathway, two of them[65, 66] also have a small bite bidentate ligand, and another one[67] with a large O-Ti-O bond angle (113°) undoubtedly due to the severe steric repulsion of the two mesitylalkoxide ligands present.
3) Some structures with $S(T_d) > 5.0$ and $S(D_{4h}) < 27$ are nicely aligned along the plier distorsion path and are seen to have bidentate diimido ligands with a bite angle of less than 90°, $[M(\{NtBu\}_2SiMe_2)_2]$ (M = Ti, Zr of Hf[68, 69]). The structure that is most distorted along the plier pathway is a perrhenate anion that has an unusual O-Re-O bond angle of 56.9° and a corresponding O···O distance of 1.9 Å.[70] Interestingly, the centroid of the two nearby oxygen atoms forms angles of around 120° with the two remaining oxo ligands, suggesting an incipient tricoordinated trigonal planar peroxo complex.

d^1 ions: This configuration also shows a clear preference for the tetrahedron, with no structure found that can be considered strongly distorted from tetrahedral. The small deviations from the ideal tetrahedron observed correspond mostly to slight flattening along the spread coordinate, as

indicated by deviation functions of a 15% of the symmetry angle $\theta(T_d, D_{4h})$ or less. The only point that shows a sizeable deviation from the spread path ($\Delta = 7.2$) corresponds to a vanadium complex with bidentate silyldiimido ligands with a small bite (N-V-N angles of 84°) and is therefore along the plier distortion path.[69] Yet the tetrahedricity of this molecule, $S(T_d) = 4.6$, allows us to classify it as a distorted tetrahedron.

d^2 ions: Again, among the d^2 electron configuration there is a marked preference for the tetrahedron, but two structures with practically planar geometry can be identified, corresponding to W^{IV} complexes with bulky phenoxide ligands.[71] Also a point can be identified along the umbrella distortion path (highest line), which corresponds to a V^{III} complex with a tetradentate tripod ligand.[72] All these compounds seem to have a triplet ground state.[73]

d^3 ions: Few structures have been found for tetracoordinate d^3 ions, but these clearly suggest that both the tetrahedron and the square are likely, whereas intermediate geometries seem to be forbidden. Among the moderately distorted tetrahedra, an umbrella-distorted molecule[74] can be easily identified. Other deviations from the tetrahedron characterized by $S(D_{4h})$ values between 15 and 25 correspond to asymmetric distortions of the tetrahedron toward the sawhorse geometry, and two of them seem to be closer to the sawhorse shape than to the tetrahedron, having S(sawhorse) values of 0.67[41] and 2.75,[42] whereas a third structure is practically equidistant to the tetrahedron and the sawhorse (shape measures of 3.47 and 3.46, respectively).[75] All but one of the practically square-planar complexes[41, 76–78] have bulky substituents (*i*Pr or *t*Bu) in the *ortho* positions of phenoxide ligands that are placed perpendicular to the coordination plane to avoid steric repulsions. The exception is $[Cr(tmen)(CH_2Ph)(CHPh)]$, and although one can wonder whether the Cr=C double bond has some influence on the choice of the square-planar geometry, it has been proposed that the presence of an agostic interaction favors such a stereochemistry.[79] Also in NbO the d^3 Nb^{II} ions have a perfectly square planar geometry.[80] We note that d^3 compounds of first-row transition metals (V and Cr) and of Mo[81] appear in the high-spin configuration (magnetic moments ~3.8 μ_B), whereas those of third row metals (Re and Os) have a low-spin configuration with one unpaired electron (magnetic moments ~1.2 μ_B); however, there seems to be no correlation between the spin state and the structural choice.

d^4 ions: The d^4 complexes show no clear structural preference, their structures being found throughout the spread pathway, including perfect tetrahedra and squares. It is remarkable that the most scissor-distorted planar molecules correspond to chelated complexes,[82, 83] although examples of scissor-distorted molecules with only monodentate ligands can be found,[84–86] including such a simple molecule as $[CrCl_4]^{2-}$. The nearly perfect tetrahedral structures found ($S(T_d)$) values smaller than 3)[87–94] all have alkyl, aryl, or thiolato ligands and appear in the low-spin configuration, according to either magnetic susceptibility measurements or the sharpness of the reported NMR spectra. In contrast, all non-tetrahedral

molecules (characterized by $S(T_d) > 5.0$) for which the magnetic moment has been measured are found in the high-spin state, with the exception of those showing intermolecular exchange interactions. Poli had already noted[73] that for d^4 organometallic complexes the square-planar geometry is preferred for high-spin compounds and the tetrahedral one for a low-spin configuration, while the present results indicate that such an asertion can be extended to both organometallic and Werner-type complexes. Finally, there are two points corresponding to a Cr^{II} complex[43] that appear at $S(T_d) \approx 10$, which could in principle correspond to either flattened tetrahedra or to sawhorse geometries (this compound does not belong to our reference structural data set because it is disordered, and its data are indicated in Figure 8 by crosses). Their small sawhorse shape measures (1.16 and 1.46) and the larger tetrahedral and square measures allow us to unambiguously classify them as sawhorse structures.

d^5 ions: As we reach the d^5 configuration, geometries intermediate between tetrahedral and square planar become again unlikely. Most structures can be classified as tetrahedra or moderately distorted tetrahedra, although a few square-planar complexes are known all of them Mn^{II},[95–103] or Fe^{III}[104] complexes, including phthalocyaninato, porphyrinato, and related complexes.[96–98, 101] A few compounds with only monodentate ligands[95, 102, 103, 105] that appeared as square planar were disregarded, since closer inspection shows them to be actually hexacoordinate. Although the magnetic behavior of such square-planar compounds has not been reported in several cases, intermediate $(S = 3/2)$[99] and high-spin $(S = 5/2)$[97] states have been identified, and it is likely that the square-planar geometries adopt the low-spin and the tetrahedral ones the high-spin configuration. Another remarkable case is that of the Ir^{IV} oxoanions in A$_4$IrO$_4$ (A = Na, K, Cs), which are perfectly square planar. Two unique cases[73] of d^5 ions with tetrahedral geometry in a low spin configuration are those of [Co(norbornyl)$_4$][106] and [Fe(N-p-tolyl){PhB(CH$_2$PPh$_2$)$_3$}].[107] This behavior is to be compared with that of [Mn(CN)$_4$]$^{2-}$, which is a high-spin compound[108] despite the strong field ligands.

d^6 ions: It has been stated that a d^6 tetracoordinate complex prefers to be in a *cis*-divacant octahedral (or sawhorse) geometry,[109] and theoretical geometry optimization on several compounds supports this assertion.[16, 109–111] Experimentally, Caulton and co-workers have made extensive use of the facility with which octahedral and sawhorse geometries can interconvert by dissociation and association of ligands, generating sawhorse structures by dehydrohalogenation of hexacoordinate complexes, as in [Ru(NO)(CO)(PMetBu$_2$)$_2$]$^+$,[112] with S(sawhorse) = 2.5, and [Ir(H)$_2$(PPhtBu$_2$)$_2$]$^+$,[113] for which the shape measures could not be calculated, because the hydrido ligands have not been located in the crystal structure. These two complexes, though, have not been included in our set of analyzed structures because they are disordered. However, the distribution of tetracoordinate d^6 structures in the symmetry map indicates that tetrahedra and square-planar structures are more common than the sawhorse. In fact, different geometrical preferences are expected for

different spin states. According to Poli,[73] the high-spin configuration prefers the tetrahedral geometry, whereas the low-spin one prefers square planar structures.

d^7 ions: For this electron configuration we find again a large number of structures close to the tetrahedron, a few of them[46–49] being better described as sawhorses according to our classification criteria (see Table 1). One must be careful, though, not to assign a sawhorse geometry based only on the corresponding shape measure, since the neglect of two *cis* ligands of an octahedral complex would always give small sawhorse shape measures. We note, for instance, that in [Co(mIm)$_2$(PhNO$_2$)$_2$][46] there are two intramolecular contacts to oxygen atoms that would complete an octahedral coordination sphere, with an octahedral symmetry measure of 0.94, clearly indicating that such compound is best described as a slightly distorted octahedron. Although the situation is less clear for other d^7 complexes (Table 1) that have larger octahedral symmetry measures, their values suggest that these compounds are along the path that goes from the octahedron to the sawhorse through dissociation of two *cis* ligands. There is also a group of structures close to the square, but there are very little structures in the middle of the tetrahedral to square-planar interconversion path (the four points in the range $11 < S(T_d) < 20$ correspond to Co^{II} complexes with N-donor macrocyclic ligands[114–116]). Such a distribution is consistent with the energy surfaces for the low- and high-spin states having different minima and both being high in energy at intermediate geometries. Indeed, Poli[73] has proposed that the high-spin quartet state prefers the tetrahedral geometry, whereas the low-spin doublet prefers square-planar structures. Lippard and co-workers[116] prepared a series of Co^{II} tropocoronand complexes with variable size of the macrocyclic ligands, achieving in this way a tuning of the stereochemistry from distorted square planar for the smaller macrocycles to distorted tetrahedral for the larger ones. These authors showed that the nearly square planar complexes have low spin, whereas the nearly tetrahedral ones have high-spin configurations. It is also worth mentioning that equilibrium in solution between the planar low-spin and tetrahedral high-spin forms in Co^{II} β-ketoiminates were reported by Everett and Holm.[117] It must be mentioned, though, that a low-spin Co^{II} compound with a distorted tetrahedral geometry (inverted umbrella distortion: $S(T_d) = 3.5$, $S(D_{4h}) = 32.4$) has been recently characterized.[118]

d^8 ions: Keinan and Avnir had previously analyzed[3] the symmetry measures corresponding to experimental structures of the [NiX$_4$]$^{2-}$ (X = Cl, CN) and [PtX$_4$]$^{2-}$ (X = halide) complexes. The [NiCl$_4$]$^{2-}$ anion was found to be always practically tetrahedral, whereas [Ni(CN)$_4$]$^{2-}$ and the tetrahaloplatinates are always nearly perfect square planar. The present analysis allows us to draw some more general conclusions. If we plot the symmetry measures for all d^8 complexes in a symmetry map (Figure 8), we see a large number of structures that can be described as tetrahedra or distorted tetrahedra, and also a great deal of square or distorted square-planar structures, while practically no structures with symmetry measures around the center of the spread

pathway can be found. However, a better description of the stereochemical preferences of d⁸ complexes can be established, since the geometry distribution for Ni^{II} and Co^{I} complexes is quite different from that for the rest of d⁸ metal ions. These two metal ions can appear as either tetrahedral (presumably in a high-spin configuration with S = 1) or square planar (in a low-spin, S = 0 configuration), as seen in Figure 9
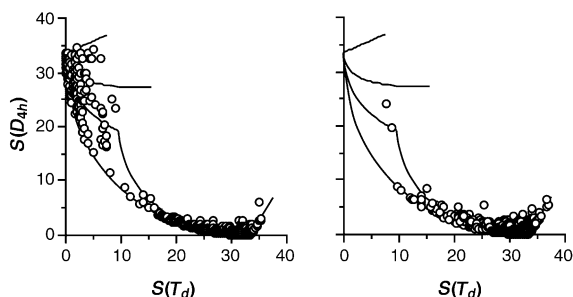

Figure 9. Continuous shape measures of experimental structures for d⁸ tetracoordinate complexes according to the central metal atom: Ni and Co (left), and all other transition metals (right).

(left). Among the tetrahedral cobalt complexes we note those that have three or four phosphine ligands. The rest of the d⁸ metal ions, including Cu^{III}, Ag^{III}, Au^{III}, Pd^{II}, Pt^{II}, Rh^{I}, Ir^{I}, Fe^{0}, and Ru^{0}, are found only (with five exceptions) in square planar geometries, although many of these compounds are severely distorted toward the tetrahedron along the spread pathway (Figure 9, right). The five exceptions correspond to sawhorse structures, including the [RuH$_4$]$^{4-}$ ion, which has two neighboring Ru atoms in the *cis* vacant octahedral positions. Even if the angles around Ru are quite close to the octahedral ones, the octahedral shape measure (Table 2) is rather high, due to the large difference in interatomic distances (Ru−H = 1.67 and Ru···Ru = 3.24 Å). One may think that the Ru−Ru distance is too long to indicate bonding (cf. an atomic radii[119] sum of 2.94 Å) consistent with an octahedral geometry, but Ru−Ru bonds larger than 3.2 Å are not uncommon in clusters, according to a CSD search. Hence, the question of whether this peculiar anion should be described as a molecular sawhorse or as a chain of vertex-sharing octahedra is still open to debate.

The structure reported for [FePh$_4$]$^{4-}$ seems to have a severe scissoring distortion (C-Fe-C bond angles of 61°),[120] but later structural redeterminations[121, 122] of that compound found the Fe atom to be hexacoordinate with regular bond angles of 90°, corresponding to the formula [FeH$_2$Ph$_4$]$^{4-}$. Although statistically of little significance, a few sawhorse structures have beeen identified, such as the Ir^{I} and Ru^{0} compounds presented in Table 2. Such an unusual structure for d⁸ compounds has also been found for the [Fe(CO)$_4$] species in its singlet transient state in the gas phase (bond angles of 169 and 125°),[123] consistent with the theoretically predicted geometry.[124, 125] A similar structure, if somewhat closer to the tetrahedron, was also proposed based on IR spectroscopy[126] and theoretically predicted[124, 125] for the triplet ground state of [Fe(CO)$_4$].

The halo–phosphine nickel complexes, [NiX$_2$(PR$_3$)$_2$], provide classical examples[127] of tetracoordinate molecules that

have stereoisomerism, appearing as either tetrahedral or square planar. Such a behavior is nicely revealed by plotting their symmetry measures in a symmetry map (Figure 10),
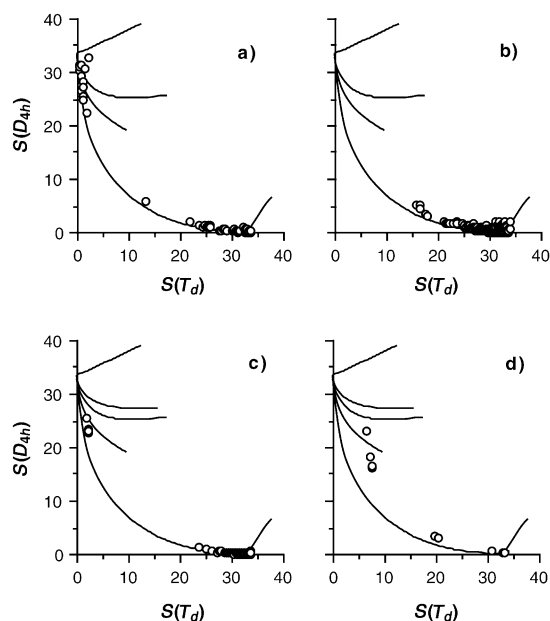

Figure 10. Symmetry map for a) Ni^{II} and b) Pd^{II} or Pt^{II} complexes with general formula [MX$_2$(PR$_3$)$_2$], and for Ni^{II} complexes with c) salycilenealdiminato and d) aminotroponeiminato ligands.

where we see most structures grouped close to the two perfect shapes. For the particular case of [NiBr$_2$(PBzPh$_2$)$_2$], two crystallographically independent molecules in the unit cell possess the two alternative structures, tetrahedral and square planar.[128] The different electronic structure of the two isomers is well reflected by the longer bond lengths in the tetrahedral (Ni−Br = 2.355, Ni−P = 2.306 Å) than in the square planar case (Ni−Br = 2.315, Ni−P = 2.262 Å). In contrast with the halocuprates analyzed above, practically no intermediate structures are found in this family of complexes (Figure 10a), the most salient example being that of a complex with binaphthyl diphosphine, [NiBr$_2$(binap)].[129]

Another family that presents both tetrahedral and square planar structures, but no strongly distorted intermediate geometries, is that of the Ni^{II} salycilenealdiminato complexes. A scatterplot of the symmetry measures for such molecules (Figure 10c) clearly shows that they appear along the tetrahedron/square-planar pathway, but only at the two extremes, that is, as tetrahedra with a small degree of planarization or as a square with a small degree of tetrahedricity, but the intermediate geometries seem to be forbidden. Aminotroponeiminato complexes of Ni^{II} have long been known to present tetrahedral/square-planar isomerism, and complexes with derivatives of such ligand were structurally characterized in the last decades.[130–133] The symmetry measures of these structures (Figure 10d) trace the path for the square planar to tetrahedral interconversion, although structures at the tetrahedral end of the path are significantly distorted due to the small bite angles (80–82°).

So far we have focused only on the square planar or tetrahedral nature of the coordination sphere, but in many square-planar complexes of the type $[ML_2X_2]$ there is a choice between *cis* and *trans* isomers. Focusing on the experimental data for the family of $[Ni(PR_3)_2X_2]$ complexes, we note that the tetrahedral, *cis*-square-planar, and *trans*-square-planar structures are found with only minor distortions, whereas no structures with significantly distorted intermediate geometries exist. This result suggests that tetrahedral intermediates for the *cis–trans* isomerization in these compounds are unlikely.

The analogous halo–phosphine Pd and Pt complexes have much less stereochemical variability, all their structures appearing around the perfect square-planar geometry, characterized by $S(D_{4h}) = 0.00$ and $S(T_d) = 33.33$ (Figure 10b). The deviations from the square can be attributed to one of three factors: 1) a spread distortion toward the tetrahedron following the model line, 2) a scissoring distortion of planar molecules, following the straight line (cf. Figure 3), or 3) combinations of the two modes. The complexes that have the largest deviations toward the tetrahedron correspond to three different types of compounds: 1) those with binaphthyldiphosphine, 2) those with *trans*-spanning diphosphines that are not long or flexible enough to adjust to a P-M-P bond angle of 180°, and 3) $[PtCl_2(PtBu_2Ph)_2]$,[134] probably for steric reasons. Apparently, there is no correlation between the size of the *trans*-chelate ring and the degree of distortion. In contrast, among the *cis* complexes there is a fair correlation between the size of the chelate ring and the P-M-P bond angle (Figure 11), which can be varied between 71 and 105° by
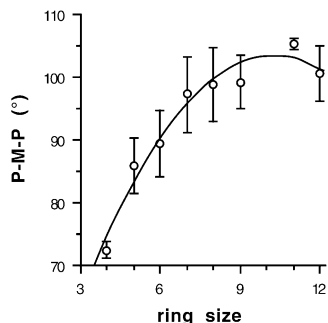
Figure 11. Relationship between the size of the chelate ring and the P-M-P bond angle for tetracoordinate Pd[II] and Pt[II] complexes with diphosphine ligands.

appropriate choice of the ligand. However, neither the size of the chelate ring nor the P-M-P bond angle show any correlation with the symmetry measures, except for the larger $S(D_{4h})$ values found for bidentate phosphines forming four-membered chelate rings (e.g., bis(diphenylphosphino)methane (dppm)), which are associated with a marked scissoring distortion (P-M-P bond angles of about 73°, X−M−X angles larger than 93°).

Finally, we have analyzed the family of Rh[I] tetraphosphine complexes. Although the d[8] Rh[I] ion prefers the square-planar geometry, a surprising variety of structures along the spread pathway are found within this family, with the deviations from planarity being probably due to large steric congestion of

monodentate phosphines or to the chelate ring strain imposed by bidentate phosphines. The scatterplot of their symmetry measures (Figure 12) allows one to detect several interesting
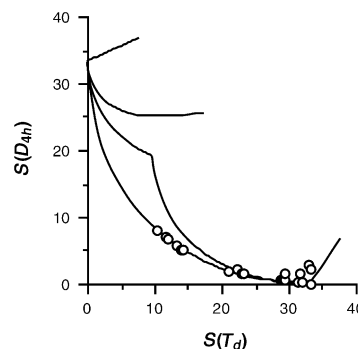
Figure 12. Symmetry map for tetraphosphine Rh[I] complexes.

features. 1) Although several structures appear to be perfectly square planar, many present significant distortions toward the tetrahedron, included complexes with PMe_3 or PMe_2Ph ($S(D_{4h}) \approx 5-7$). 2) Two complexes are perfectly planar but with a scissoring distortion induced by the small bite bidentate phosphine dppm.[135] An unusual perfectly tetrahedral structure is found[136] for $[Rh(PPh_3)_4]^+$, although it is not shown in Figure 12 due to the presence of disorder in the crystal structure. It is also worth mentioning here that other tetrahedral tetraphosphine Rh complexes are known for oxidation states Rh[0] and Rh[−I].[137, 138]

d[9] ions: Keinan and Avnir analyzed[3] the symmetry measures corresponding to experimental structures of the tetrahalocuprate(II) complexes, $[CuX_4]^{2-}$ (X = Cl, Br), and found them scattered through the spread pathway. Through Hartree–Fock calculations, these authors also showed that the spread pathway corresponds to the least energy path in the case of $[CuCl_4]^{2-}$, with the global minimum appearing for a distorted tetrahedron. According to the theoretical prediction, the perfectly square-planar structure that corresponds to $S(T_d) \approx 33.33$ has sufficiently high energy to be forbidden, in contrast with the finding of a significantly large number of Cu[II] complexes with that geometry. A closer look at these structures shows that some of them[139–142] have contacts between the Cu atom and nearby Lewis bases at less than 3.0 Å, indicating that they are best described as Jahn–Teller distorted hexacoordinate rather than as square-planar tetra-coordinate complexes. The rest of the nearly square-planar structures[142–149] possess hydrogen bonding to the coordinated halides. In summary, we can say that the probability of the molecular geometries is inversely related to their energies relative to the minimum for the isolated molecule, but weak coordination of additional ligands or hydrogen bonding can eventually favor a structure with relatively high energy. It is interesting to note that in several cases crystallographically independent anions in the same crystal structure present quite different geometries.[144, 147, 149–151] It is worth noting that for d[9] ions other than Cu[II] the tetrahedral geometry is found in only one out of 26 structures, corresponding to a biquinolyl Co[0]

compound,[152] but the remaining structures found are per-
fectly or slightly distorted square planar.

d¹⁰ ions: The distribution of the d¹⁰ ions in the symmetry map
indicates a clear preference for the tetrahedron, in agreement
with the 18-electron rule, although a good number of
molecules appear to be severely distorted from the tetrahe-
dron. Although we do not intend to analyze here all the
deviations from the typical behavior, we note that the three
outliers at the top of the plot correspond to two compounds
with severe umbrella distortions produced by the tridentate
1,3,5-triazacyclohexane ligand (N–Cu–N bond angles of
about 63°).[40, 153]

Among the compounds that are practically square planar,
we find complexes with porphyrin or other macrocyclic
ligands, mostly Zn^{II}, as discussed above (see Figure 6). Other
square-planar complexes have relatively rigid tri- or tetra-
dentate open chain ligands.[154] The exceptions to this rule are
a $Cu^{I[155]}$ and a $Ag^{I[156]}$ compound with two bidentate ligands
each. A number of Cd^{II} and Hg^{II} complexes that appeared as
square planar were disregarded, since closer inspection of
their structures showed that they were actually bicoordinated
with two donor atoms at significantly longer distances (usually
corresponding to potentially bidentate ligands that coordinate
as monodentate). Although many d¹⁰ complexes appear in the
symmetry map in the region of the sawhorse, the correspond-
ing shape measure, S(sawhorse), is larger than 6 in all cases,
indicating that these structures are plier-distorted tetrahedra
due to the small normalized bite (1.21) of the bidentate
ligands analyzed.

Corollary: The stereochemical choice of tetracoordinate
complexes for the different electron configurations can be
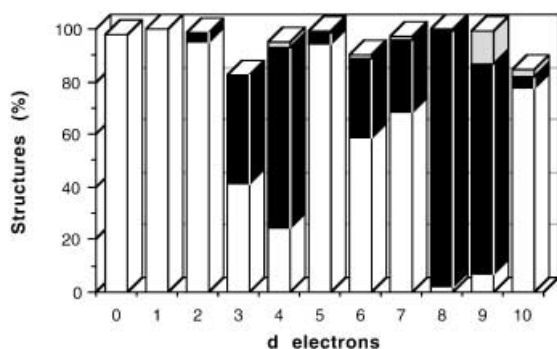summarized in Figure 13. There we can see that:

Figure 13. Distribution of the structures of tetracoordinate complexes
according to the electron configuration of the metal atom: white for
tetrahedral, black for square planar, and gray for intermediate structures
along the spread pathway. The percentage of structures missing to reach
100 % correspond to either sawhorse or unassigned structures (see
Table 1).

1) The transition-metal complexes with electron configura-
tions d⁰, d¹, d², d⁵, and d¹⁰ show a marked preference for the
tetrahedral geometry.
2) Those with d⁸ and d⁹ configurations have a strong tendency
to be square planar.

3) Complexes of d³, d⁴, d⁶, and d⁷ metals have significant
proportions of both tetrahedral and square planar struc-
tures.
4) An important fraction of structures intermediate between
square planar and tetrahedral is found for d⁹ ions.
5) A significant number of structures that cannot be ade-
quately described as tetrahedral, square planar or inter-
mediate is found for d³, d⁶, and d¹⁰ electron configurations.

Influence of the ligands on the coordination sphere: To
analyze the possible influence of the ligands on the stereo-
chemistry of the coordination sphere we have further
analyzed the structures of each electron configuration by
the ligand denticity, considering only homoleptic complexes.

Complexes with bidentate ligands: Throughout the present
section we will characterize the coordinated bidentate ligands
by their most relevant structural parameter, the *normalized
bite*, defined as the ratio between the donor–donor distance
and the average metal–donor distance. Although such a
parameter is in fact characteristic of a given ligand–metal
pair, changes in atomic size along the first transition-metal
series are small enough as to consider average values for those
metals as a metric parameter of the ligand to a good
approximation. The following bidentate ligands were consid-
ered, allowing for all substitution patterns of the basic
skeleton: bipyridine, ethylenediamine, β-diketonates, dithio-
carbamates, dithiolenes, diphosphinomethane (e.g., dppm),
diphosphinoethane (e.g., 1,2-bis(diphenylphosphino)eth-
ane(dppe)) and *vic*-dioximes. Small bite bidentate ligands
(diphosphinomethanes and dithiocarbamates) appear only
(30 structural data) in the square-planar geometry, a fact that
should be associated to ligand rigidity, since the ideal
normalized bite is 1.63 for tetrahedral bond angles, but 1.41
for a square. Ligands with larger bites (ethylenediamine,
bipyridine, dithiolates) seem to adapt well to all structural
situations among the square and tetrahedral extremes. If we
focus on the statistically more significant data for d⁸, d⁹, and
d¹⁰ complexes, we find the same general trends discussed
above for complexes with those electron configurations: d⁸
compounds appear in square-planar geometry, most d⁹ com-
plexes have nearly square-planar structures, but some deviate
from the perfect square as the ligand's normalized bite differs
from ideality (1.41), thus imposing a scissoring distortion,
nicely following the model curves. Other d⁹ compounds
(empty circles in Figure 14), though, deviate from the model
curve and represent snapshots along the twist pathway (a
change in the torsion angle from 0 to 90° while keeping two
bond angles subtended by bidentate ligands constant),
approaching the tetrahedron without significant changes in
their normalized bites. Finally, most d¹⁰ complexes appear
close to the tetrahedron, with the ligand bite enforcing a plier
distortion (points along the parabola in Figure 14).

Complexes with tridentate ligands: The symmetry behavior of
tetracoordinate complexes with the following tridentate
ligands was analyzed: 1) ligands with donor atoms that favor
a meridional conformation, such as terpyridine and the so-
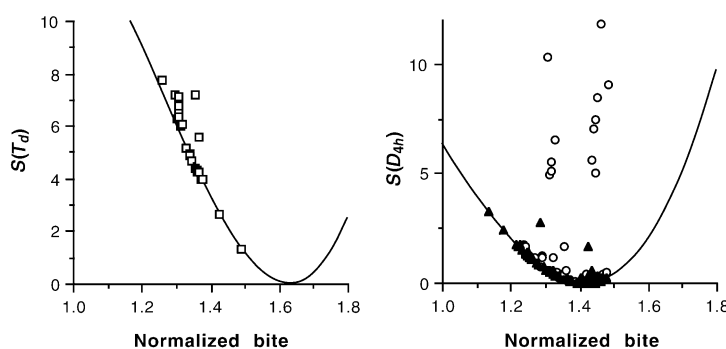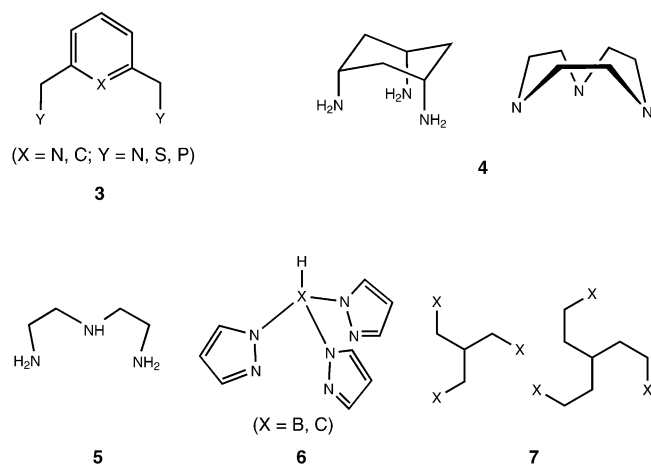called pincers (3), 2) cyclic ligands that favor facial coordi-

Figure 14. Continuous symmetry measures as a function of the normalized bite of two bidentate ligands in bischelate metal complexes: tetrahedricity with plier distortion (left) and square planarity with scissoring (right). The continuous lines correspond to model curves, squares (left) to d^{10} complexes, triangles and circles (right) to d^8 and d^9 complexes, respectively.

nation, such as cyclohexanetriamine or triazacyclononane (**4**), and 3) ligands topologically analogous to **3** or **4**, but with more flexible skeletons (e.g., diethylenetriamine, **5**), including tris(pyrazolyl)borate (**6**) and the triskelion ligands (**7**, from the Greek *skelos*, leg: a symbolic figure of three legs or lines from a common centre).

ligands. Let us note here that a few cases[43, 157–159] of compounds with electron configurations other than d^8 –d^{10} and with tridentate ligands of type **6** were found above to correspond to sawhorse geometries.

Facial coordinating ligands **4** appear only in tetrahedral complexes, if distorted along the umbrella pathway (Scheme 2). A representation of the tetrahedral symmetry measures as a function of the pyramidality angle β for the macrocyclic tridentate ligand 1,4,7-triazacyclononane (TACN) (Figure 15) shows that the umbrella distortion is
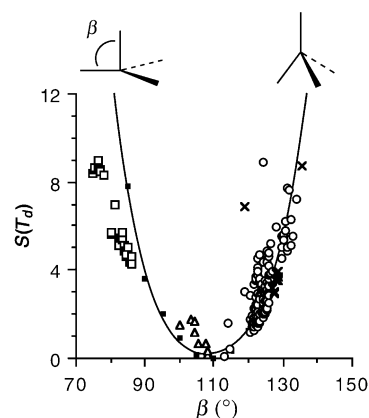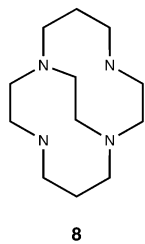

Figure 15. Dependence of the tetrahedricity on the axial bond angle in tetracoordinate complexes with tri- and tetradentate ligands that favor umbrella distortions: triskelions with three- (circles) and four-atom (triangles) legs, triazacyclononane (squares) and tetradentate tripods (crosses). The solid line corresponds to a model distortion keeping the C_{3v} symmetry.

responsible for most of the loss of tetrahedricity. The only one case that shows a significant deviation along the off-axis (see Scheme 2) displacement curve in Figure 3 corresponds to a complex[160] in which the TACN macrocycle has a pendant arm that occupies the fourth coordination position and is forced to an off-axis distortion.

Complexes with tetradentate ligands: Among the complexes with tetradentate ligands we have analyzed the families that have tripod or macrocyclic (cyclam, porphyrins, or phthalocyanines) ligands. In complexes with tripod ligands, given the short distance between the apex and the foot of the tripod, the bond angles β are rather small (Figure 15), since larger angles impose too short distances from the metal to the apical donor atom. As a result, they experience an umbrella distortion from the ideal tetrahedron, opposite to that discussed for the tridentate triskelion ligands, but with a similar loss of tetrahedricity at a quantitative level.

Our results for complexes with macrocyclic ligands indicate that the square-planar geometry is enforced in all cases. However, in contrast to porphyrins and phthalocyanines, the flexibility of cyclam allows it to adapt to nonplanar geometries, and significant spread distortions can be found for d^9 complexes with that ligand. Of the two outliers in Figure 15, one corresponds to a Cu^{II} complex,[161] which differs from other Cu^{II} complexes with the same ligand that are practically

Meridional ligands of types **3** and **5** do not give tetrahedral structures, but significant distortions along the spread pathway are found for the d^{10} ions, reflecting the marked preference of this electron configuration for the tetrahedron. Conversely, complexes with facial ligands of types **4**, **6**, and **7** are found to appear only with nearly tetrahedral structures, with the only exception of the two sawhorse structures discussed above (Table 2). If we compare the results for triskelion ligands **7** with legs of different lengths, we find that those with longer legs allow for a better adaption to the tetrahedral angles around the metal atom and the resulting complexes are nearly perfect tetrahedral, whereas those with shorter legs are more distorted. We also observe that the symmetry measures reflect the higher rigidity of the macrocyclic tridentate ligands compared to that of the triskelion

square planar. The second outlier corresponds to a Cu[I] complex[56] with a sawhorse geometry, forced by the existence of a tether between two intended *trans* N-donor atoms of the cyclam skeleton (**8**). It is appropriate to recall here what we found for Zn[II] and Cd[II] complexes with tropocoronands (**2**), which can be found in different geometries between square planar and nearly tetrahedral, depending on the length of the side chains (Figure 6). Remarkably, the same behavior is found for other divalent metal ions (Co, Ni, and Cu), with practically the same linear relationship between the square planar symmetry measure and the combined chain length. Furthermore, for Co[II] and Ni[II] the distortion from square planar to tetrahedral is accompannied by a change in the spin state.[116, 131, 162]

8

Conclusion

In this contribution we have presented the symmetry map for tetracoordination, showing the wedge-shaped geometrically allowed region and the chemically inhabitable region, the lower portion of the symmetry map, occupied by the set of more than 13000 tetracoordinate transition-metal centers analyzed. The positions of several distortions of the tetrahedron and of the square in the symmetry map have been identified, and the possibility of using such map to detect relevant distortions in large data sets has been discussed.

A structural classification of the teetracoordinate complexes analyzed has been performed by using the tetrahedral and square-planar symmetry measures. Most of the structures have been found to be close to square planar (72%) or nearly tetrahedral (23%). A large part of the unassigned structures can be described as intermediate along the spread pathway for the interconversion of the tetrahedron and the square by evaluating the corresponding deviation function (3%). The possibility of using the sawhorse as a reference shape is evaluated and found to be useful, not only to detect the *cis*-divacant geometry, but also to detect structures that can be better described as linear with two additional interactions (found for a significant portion of the putative tetracoordinate Hg[II] compounds), or as a fragment of an octahedral or a trigonal-bipyramidal complex.

The distribution of tetracoordination throughout the transition-metal series has been analyzed, showing that tetrahedral complexes are found for all such metals, the most common ones corresponding to the members of Groups 9–12, while very little or no square-planar structures at all are found for vanadium and the second and third transition series elements of Groups 3–8.

An analysis of the structures by metal electron configuration allows us to extract some general trends: 1) d[0], d[1], d[2], d[5], and d[10] configurations prefer the tetrahedral geometry; 2) d[8] and d[9] complexes show a strong preference for the square-planar geometry; 3) d[3], d[4], d[6], and d[7] metals appear in both

tetrahedral and square-planar structures; 4) a significant fraction d[9] ions have structures intermediate between square planar and tetrahedral; and 5) a large number of structures that cannot be adequately described as tetrahedral, square planar or intermediate is found for d[3], d[6], and d[10] complexes.

Stereochemical preferences for several families of complexes with bi-, tri-, and tetradentate ligands have also been analyzed. Bidentate ligands with small normalized bites (dithiocarbamates and dppm) appear only in square-planar geometry, whereas ligands with larger bites (ethylenediamine, bipyridine, and dithiolates) can adapt to both tetrahedral and square-planar coordination spheres. Tridentate ligands adapted for meridional coordination have not been found in tetrahedral structures, while those best suited for facial coordination appear only with nearly tetrahedral structures. Among the tetradentate ligands, tripods are found only in tetrahedral complexes with significant umbrella distortions. Rigid macrocyclic tetradentate ligands such as porphyrins or phthalocyanines enforce square-planar coordination even for those electron configurations that show a marked preference for the tetrahedral geometry. Added flexibility present in the backbone of cyclam allows for significant distortions toward the tetrahedron, with the resulting intermediate geometries being a compromise between the preference of the ligand for planarity and the electronic preference of the metal atom for tetrahedricity. Macrocyclic ligands with extra flexibility provided by increasing lengths of the aliphatic linkers between donor atoms, such as the tropocoronands, provide excellent control of the degree of tetrahedricity around the metal atom.

Acknowledgements

Appendix

The collection of structural data was obtained through systematic searches of the Cambridge Structural Database[163] (version 5.23). General searches for tetracoordinate transition-metal complexes were carried out allowing single, double, or triple bonds to donor atoms from periodic Groups 14–17, excluding direct bonds between donor atoms, constraining the search to non-polymeric structures with no disorder, *R* factors of at most 0.10, and excluding di- and polynuclear complexes. From all the structures retrieved, only those for which the metal oxidation state (not amenable to systematic search in the structural databases) could be unambiguously assigned were retained. The analysis of continuous shape measures by electron configuration was restricted to complexes with metal–ligand single, double, or triple bonds. The searches for $[CuX_4]^{2-}$ included all mononuclear compounds with X = F, Cl, Br, or I, and no disorder. From the family of $[M(bipy)_2]$ compounds, those with M = Cu[II] or Ag[II] with short contacts to atoms of Groups 6 or 7 were excluded, since deviations from the general trends found should be attributed to their coordination number larger than four. Structures were also retrieved from the inorganic database (ICSD), especially for isolated anions in alkaline or alkaline-earth salts, but the

search is far from comprehensive in this case, since connectivity searches are not implemented in the ICSD. The shape and symmetry measures were calculated with the *sym_he* program of Pinsky and Avnir and with SHAPE (version 1.1), a program developed in our group.[164]

[1] R. H. Crabtree, *The Organometallic Chemistry of the Transition Metals*, Wiley, New York, **2001**.

[2] D. F. Shriver, P. W. Atkins, *Inorganic Chemistry*, 3rd ed., Oxford University Press, Oxford, **1999**.

[3] S. Keinan, D. Avnir, *Inorg. Chem.* **2001**, *40*, 318.

[4] S. Alvarez, D. Avnir, *J. Chem. Soc. Dalton Trans.* **2003**, 562.

[5] M. Elian, R. Hoffmann, *Inorg. Chem.* **1975**, *14*, 1058.

[6] J. K. Burdett, *Molecular Shapes. Theoretical Models of Inorganic Stereochemistry*, Wiley, New York, **1980**.

[7] T. A. Albright, J. K. Burdett, M.-H. Whangbo, *Orbital Interactions in Chemistry*, Wiley, New York, **1985**.

[8] H. Zabrodsky, S. Peleg, D. Avnir, *J. Am. Chem. Soc.* **1992**, *114*, 7843.

[9] D. Avnir, O. Katzenelson, S. Keinan, M. Pinsky, Y. Pinto, Y. Salomon, H. Zabrodsky Hel-Or, in *Concepts in Chemistry: A Contemporary Challenge* (Ed.: D. H. Rouvray), Research Studies Press, Taunton (UK), **1996**.

[10] S. Alvarez, D. Avnir, M. Llunell, M. Pinsky, *New J. Chem.* **2002**, *26*, 996.

[11] S. Alvarez, M. Llunell, *J. Chem. Soc. Dalton Trans.* **2000**, 3288.

[12] D. Casanova, J. M. Bofill, P. Alemany, S. Alvarez, *Chem. Eur. J.* **2003**, *9*, 1281.

[13] M. Pinsky, D. Avnir, *Inorg. Chem.* **1998**, *37*, 5575.

[14] D. Casanova, P. Alemany, J. Cirera, S. Alvarez, unpublished redsults.

[15] H. Zabrodsky, S. Peleg, D. Avnir, *J. Am. Chem. Soc.* **1993**, *115*, 8278.

[16] G. Ujaque, A. C. Cooper, F. Maseras, O. Eisenstein, K. C. Caulton, *J. Am. Chem. Soc.* **1998**, *120*, 361.

[17] D. Huang, W. E. Streib, O. Eisenstein, K. C. Caulton, *Organometallics* **2000**, *19*, 1967.

[18] Y.-S. Wong, A. J. Carty, P. C. Chieh, *J. Chem. Soc. Dalton Trans.* **1977**, 1157.

[19] K. Lewinski, J. Sliwinski, L. Lebioda, *Inorg. Chem.* **1983**, *22*, 2339.

[20] C. Chieh, *Can. J. Chem.* **1977**, *55*, 1583.

[21] A. J. Canty, N. J. Minchin, B. W. Skelton, A. H. White, *J. Chem. Soc. Dalton Trans.* **1986**, 2301.

[22] D. A. House, V. McKee, W. T. Robinson, *Inorg. Chim. Acta* **1989**, *157*, 15.

[23] A. Linden, B. D. James, J. Liesegang, N. Gonis, *Acta Crystallogr. Sect. B* **1999**, *55*, 396.

[24] R. C. Larock, L. D. Burns, S. Varaprath, C. E. Russell, J. W. Richardson, Jr., M. N. Janakiraman, R. A. Jacobson, *Organometallics* **1987**, *6*, 1780.

[25] A. L. Poznyak, I. F. Burshtein, *Zh. Neorg. Khim.* **1999**, *44*, 1459.

[26] H. Terao, M. Hashimoto, T. Okuda, A. Weiss, *Z. Naturforsch. Teil A* **1998**, *54*, 559.

[27] R. Weiss, N. Kraut, F. Hampel, *J. Organomet. Chem.* **2001**, *617*, 473.

[28] A. B. Salah, J. W. Bats, R. Kalus, H. Fuess, A. Daoud, *Z. Anorg. Allg. Chem.* **1982**, *493*, 178.

[29] A. C. Cooper, E. M. Gopalakrishna, D. A. Norton, *Acta Crystallogr. Sect. B* **1968**, *24*, 935.

[30] R. Carballo, A. Castiñeiras, T. Pérez, *Z. Naturforsch. Teil B* **2001**, *56*, 881.

[31] Z. Popovic, G. Pavlovic, D. Matkovic-Calogovid, Z. Soldin, M. Rajic, D. Vikic-Topic, D. Kovacek, *Inorg. Chim. Acta* **2000**, *306*, 142.

[32] I. A. Tikhonova, F. M. Dolgushin, A. I. Tanovsky, Z. A. Starikova, P. V. Petrovskii, G. G. Furin, V. B. Shur, *J. Organomet. Chem.* **2000**, *613*, 60.

[33] A. J. Blake, S. Parsons, C. Radek, M. Schroder, *Acta Crystallogr. Sect. C* **1996**, *52*, 21.

[34] R. Kaur, H. B. Singh, R. P. Patel, S. K. Kulshreshtha, *J. Chem. Soc. Dalton Trans.* **1996**, 461.

[35] N. A. Bell, M. Goldstein, L. A. March, I. W. Nowell, *J. Chem. Soc. Dalton Trans.* **1984**, 1621.

[36] P. Chaudhuri, M. Hess, K. Hildenbrand, E. Bill, T. Weyhermuller, K. Wieghardt, *Inorg. Chem.* **1999**, *38*, 2781.

[37] L. H. Doerrer, S. J. Lippard, *Inorg. Chem.* **1997**, *36*, 2554.

[38] P. Chaudhuri, M. Hess, J. Muller, K. Hildenbrand, E. Bill, T. Weyhermuller, K. Wieghardt, *J. Am. Chem. Soc.* **1999**, *121*, 9599.

[39] M. G. B. Drew, C. J. Harding, O. W. Howarth, Q. Lu, D. J. Marrs, G. G. Morgan, V. McKee, J. Nelson, *J. Chem. Soc. Dalton Trans.* **1996**, 3021.

[40] R. D. Kohn, G. Seifert, G. Kociok-Kohn, *Chem. Ber.* **1996**, *129*, 1327.

[41] R. K. Minhas, J. J. H. Edema, S. Gambarotta, A. Meetsma, *J. Am. Chem. Soc.* **1993**, *115*, 6710.

[42] B. Menjón, J. Forniés, **2002**, personal communication.

[43] J. L. Kersten, R. R. Kucharczyk, G. P. A. Yap, A. L. Rheingold, K. H. Theopold, *Chem. Eur. J.* **1997**, *3*, 1668.

[44] W. Baratta, E. Hertweck, P. Rigo, *Angew. Chem.* **1999**, *111*, 1733; *Angew. Chem. Int. Ed.* **1999**, *38*, 1629.

[45] D. Huang, W. E. Streib, J. C. Bollinger, K. C. Caulton, R. F. Winter, T. Scheiring, *J. Am. Chem. Soc.* **1999**, *121*, 8087.

[46] R. G. Little, *Acta Crystallogr. Sect. B* **1979**, *35*, 2398.

[47] D. Ulku, M. N. Tahir, N. Kesici, D. Isci, D. Kisakurek, *Z. Kristallogr. New Cryst. Struct.* **1997**, *212*, 493.

[48] J. Castro, S. Cabaleiro, P. Pérez-Lourido, J. Romero, J. A. García-Vázquez, A. Sousa, *Polyhedron* **2001**, *20*, 2329.

[49] B. B. Miminoshvili, A. E. Shvelashvili, T. O. Vardosanidze, *Zh. Neorg. Khim.* **1996**, *41*, 2066.

[50] F. Bonhomme, K. Yvon, G. Triscone, K. Jansen, G. Auffermann, P. Mueller, W. Brönger, P. Fischer, *J. Alloys Compd.* **1992**, *178*, 161.

[51] D. M. Lunder, E. B. Lobkovsky, W. E. Streib, K. C. Caulton, *J. Am. Chem. Soc.* **1991**, *113*, 1837.

[52] P. G. Edwards, F. Ingold, S. J. Coles, M. B. Hursthouse, *Chem. Commun.* **1998**, 545.

[53] H. K. Lee, Y. Peng, S. C. F. Kui, Z.-Y. Zhang, Z.-Y. Zhou, T. C. W. Mak, *Eur. J. Inorg. Chem.* **2000**, 2159.

[54] M. Ogasawara, S. A. Macgregor, W. E. Streib, K. Folting, O. Eisenstein, K. G. Caulton, *J. Am. Chem. Soc.* **1995**, *117*, 8869.

[55] M. Ogasawara, S. A. Macgregor, W. E. Streib, K. Folting, O. Eisenstein, K. G. Caulton, *J. Am. Chem. Soc.* **1996**, *118*, 10189.

[56] T. J. Hubin, N. W. Alcock, D. H. Busch, *Acta Crystallogr. Sect. C* **2000**, *56*, 37.

[57] E. Guermen, E. Daniels, J. S. King, *J. Chem. Phys.* **1971**, *55*, 1093.

[58] Z. Wu, J. B. Diminnie, Z. Xue, *Inorg. Chem.* **1998**, *37*, 6366.

[59] Z. Wu, L. H. McAlexander, J. B. Diminnie, Z. Xue, *Organometallics* **1998**, *17*, 4853.

[60] Y. E. Ovchinnikov, V. A. Igonin, T. B. Timofeeva, S. V. Lindeman, Y. T. Struchkov, M. V. Ustinov, D. A. Bravo-Zhivotovskii, *Metalloorg. Khim.* **1992**, *5*, 1154.

[61] R. E. Marsh, *Acta Crystallogr. Sect. B* **1997**, *53*, 317.

[62] L. H. McAlexander, M. Hung, L. Li, J. B. Diminnie, Z. Xue, G. A. P. Yap, A. L. Rheingold, *Organometallics* **1996**, *15*, 5231.

[63] R. H. Heyn, W. D. Tilley, *Inorg. Chem.* **1989**, *28*, 1768.

[64] Y. E. Ovchinnikov, Y. T. Struchkov, M. V. Ustinov, M. G. Voronkov, *Izv. Akad. Nauk. SSSR Ser. Khim.* **1993**, 1473.

[65] R. P. Planalp, R. A. Andersen, A. Zalkin, *Organometallics* **1983**, *2*, 16.

[66] T. H. Warren, R. R. Schrock, W. M. Davis, *Organometallics* **1998**, *17*, 308.

[67] V. M. Visciglio, P. E. Fanwick, I. P. Rothwell, *Acta Crystallogr. Sect. C* **1994**, *50*, 896.

[68] D. J. Brauer, H. Burger, E. Essig, W. Geschwandtner, *J. Organomet. Chem.* **1980**, *190*, 343.

[69] D. J. Brauer, H. Burger, G. R. Liewald, J. Wilke, *J. Organomet. Chem.* **1986**, *310*, 317.

[70] F. A. Cotton, J. Lu, Y. Huang, *Inorg. Chem.* **1996**, *35*, 1839.

[71] M. L. Listemann, R. R. Schrock, J. C. Dewan, R. M. Kolodziej, *Inorg. Chem.* **1988**, *27*, 264.

[72] C. Rosenberger, R. R. Schrock, W. M. Davis, *Inorg. Chem.* **1997**, *36*, 123.

[73] R. Poli, *Chem. Rev.* **1996**, *96*, 2135.

[74] S. Schneider, A. C. Filippou, *Inorg. Chem.* **2001**, *40*, 4673.

[75] P. J. Alonso, L. R. Falvello, J. Forniés, M. A. García-Monforte, A. Martín, B. Menjón, G. Rodríguez, *Chem. Commun.* **1998**, 1721.

[76] I. M. Gardiner, M. A. Bruck, D. E. Wigley, *Inorg. Chem.* **1989**, *28*, 1769.

[77] I. M. Gardiner, M. A. Bruck, P. A. Wexler, D. E. Wigley, *Inorg. Chem.* **1989**, *28*, 3688.

[78] M. J. Scott, W. C. A. Willisch, W. H. Armstrong, *J. Am. Chem. Soc.* **1990**, *112*, 2429.

[79] S. Hao, J.-I. Song, P. Berno, S. Gambarotta, *Organometallics* **1994**, *13*, 1326.

[80] A. L. Bowman, T. C. Wallace, J. L. Yarnell, R. G. Wenzel, *Acta Crystallogr.* **1966**, *21*, 843.

[81] C. E. Laplaza, M. J. A. Johnson, J. C. Peters, A. L. Odom, E. Kim, C. Cummins, G. N. George, I. J. Pickering, *J. Am. Chem. Soc.* **1996**, *118*, 8623.

[82] S. H. Hao, S. Gambarotta, C. Bensimon, J. J. H. Edema, *Inorg. Chim. Acta* **1993**, *213*, 65.

[83] M. B. Hursthouse, K. J. Izod, M. Motevalli, P. Thornton, *Polyhedron* **1996**, *15*, 135.

[84] J. Jubb, l. F. Larkworthy, G. A. Leonard, D. C. Povey, B. J. Tucker, *J. Chem. Soc. Dalton Trans.* **1989**, 1631.

[85] M. A. Babar, M. F. C. Ladd, l. F. Larkworthy, D. C. Povey, K. J. Proctor, L. J. Summers, *J. Chem. Soc. Chem. Commun.* **1981**, 1046.

[86] J. T. Anhaus, T. P. Kee, M. H. Schofield, R. R. Schrock, *J. Am. Chem. Soc.* **1990**, *112*, 1642.

[87] R. S. Hay-Motherwell, G. Wilkinson, B. Hussain-Bates, M. B. Hursthouse, *J. Chem. Soc. Dalton Trans.* **1992**, 3477.

[88] P. Stavropoulos, P. D. Savage, R. P. Tooze, G. Wilkinson, B. Hussain, M. Motevalli, M. B. Hursthouse, *J. Chem. Soc. Dalton Trans.* **1987**, 557.

[89] R. P. Tooze, P. Stavropoulos, M. Motevalli, M. B. Hursthouse, G. Wilkinson, *J. Chem. Soc. Chem. Commun.* **1985**, 1139.

[90] P. D. Savage, G. Wilkinson, M. Motevalli, M. B. Hursthouse, *J. Chem. Soc. Dalton Trans.* **1988**, 669.

[91] S.-L. Soong, J. H. Hain, M. Millar, S. A. Koch, *Organometallics* **1988**, *7*, 556.

[92] J. Kozelka, P. Legzdins, S. J. Rettig, K. M. Smith, *Organometallics* **1997**, *16*, 3569.

[93] E. W. Jandciu, J. Kozelka, P. Legzdins, S. J. Rettig, K. M. Smith, *Organometallics* **1999**, *18*, 1994.

[94] R. S. Hay-Motherwell, G. Wilkinson, B. Hussain-Bates, M. B. Hursthouse, *Polyhedron* **1993**, *12*, 2009.

[95] B. J. Gunderman, P. J. Squattrito, S. N. Dubey, *Acta Crystallogr. Sect. C* **1996**, *52*, 1131.

[96] J. F. Kirner, C. A. Reed, W. R. Scheidt, *J. Am. Chem. Soc.* **1977**, *99*, 1093.

[97] G. Ricciardi, A. Bencini, A. Bavoso, A. Rosa, F. Lelj, *J. Chem. Soc. Dalton Trans.* **1996**, 3243.

[98] B. N. Figgis, E. S. Kucharski, G. A. Williams, *J. Chem. Soc. Dalton Trans.* **1980**, 1515.

[99] R. Mason, G. A. Williams, P. E. Fielding, *J. Chem. Soc. Dalton Trans.* **1979**, 676.

[100] J. F. Kirner, W. Dow, W. R. Scheidt, *Inorg. Chem.* **1976**, *15*, 1685.

[101] R. Thirumurugan, S. S. S. Raj, G. Ghanmugam, H.-K. Fun, J. Manonmani, M. Kandaswamy, *Acta Crystallogr. Sect. C* **1999**, *55*, 1218.

[102] T. Glowiak, W. Sawka-Dobrowolska, *Acta Crystallogr. Sect. B* **1977**, *33*, 2763.

[103] M. Ciampolini, C. Mengozzi, P. Orioli, *J. Chem. Soc. Dalton Trans.* **1975**, 2051.

[104] D. Jacoby, C. Floriani, A. Chiesi-Villa, C. Rizzoli, *J. Chem. Soc. Chem. Commun.* **1991**, 220.

[105] A. Erdonmez, D. Ulku, *Z. Kristallogr.* **1983**, *165*, 241.

[106] E. K. Byrne, K. H. Theopold, *J. Am. Chem. Soc.* **1989**, *111*, 3887.

[107] S. D. Brown, T. A. Betley, J. C. Peters, *J. Am. Chem. Soc.* **2003**, *125*, 322.

[108] J. S. Miller, *Angew. Chem.* **1998**, *110*, 813; *Angew. Chem. Int. Ed.* **1998**, *37*, 781.

[109] M. Oliván, E. Clot, O. Eisenstein, K. C. Caulton, *Organometallics* **1998**, *17*, 3091.

[110] D. Huang, J. C. Huffman, J. C. Bollinger, O. Eisenstein, K. C. Caulton, *J. Am. Chem. Soc.* **1997**, *119*, 7398.

[111] D. Huang, W. E. Streib, O. Eisenstein, K. C. Caulton, *Angew. Chem.* **1997**, *109*, 2096; *Angew. Chem. Int. Ed. Engl.* **1997**, *36*, 2004.

[112] M. Ogasawara, D. Huang, W. E. Streib, J. C. Huffman, N. Gallego-Planas, F. Maseras, O. Eisenstein, K. C. Caulton, *J. Am. Chem. Soc.* **1997**, *119*, 8642.

[113] A. C. Cooper, W. E. Streib, O. Eisenstein, K. C. Caulton, *J. Am. Chem. Soc.* **1997**, *119*, 9069.

[114] K. A. Goldsby, A. J. Jircitano, D. L. Nosco, J. C. Stevens, D. H. Busch, *Inorg. Chem.* **1990**, *29*, 2523.

[115] R. G. Khoury, M. O. Senge, J. E. Colchester, K. M. Smith, *J. Chem. Soc. Dalton Trans.* **1996**, 3937.

[116] B. S. Jaynes, L. H. Doerrer, S. Liu, S. J. Lippard, *Inorg. Chem.* **1995**, *34*, 5735.

[117] G. W. Everett Jr., R. H. Holm, *J. Am. Chem. Soc.* **1965**, *87*, 5266.

[118] D. M. Jenkins, A. J. Di Bilio, M. J. Allen, T. A. Betley, J. C. Peters, *J. Am. Chem. Soc.* **2002**, *124*, 15336.

[119] A. A. Palacios, G. Aullón, P. Alemany, S. Alvarez, *Inorg. Chem.* **2000**, *39*, 3166.

[120] T. A. Bazhenova, R. M. Lobkovskaya, R. P. Shibaeva, A. E. Shilov, A. K. Shilova, *J. Organomet. Chem.* **1983**, *244*, 265.

[121] T. A. Bazhenova, L. M. Kachapina, A. E. Shilov, M. Y. Antipin, Y. T. Struchkov, *J. Organomet. Chem.* **1992**, *428*, 107.

[122] J. M. Jefferis, G. S. Girolami, *Organometallics* **1998**, *17*, 3630.

[123] H. Ihee, J. Cao, A. H. Zewail, *Angew. Chem.* **2001**, *113*, 1580; *Angew. Chem. Int. Ed.* **2001**, *40*, 1532.

[124] O. González-Blanco, V. Branchadell, *J. Chem. Phys.* **1999**, *110*, 778.

[125] T. Ziegler, V. Tschinke, L. Fan, A. D. Becke, *J. Am. Chem. Soc.* **1989**, *111*, 9177.

[126] M. Poliakoff, J. Turner, *J. Chem. Soc. Dalton Trans.* **1974**, 2276.

[127] C. R. C. Cousmaker, M. H. Hutchinson, J. R. Mellor, L. E. Sutton, L. M. Venanzi, *J. Chem. Soc.* **1961**, *3*, 2705.

[128] B. T. Kilbourn, H. M. Powell, *J. Chem. Soc. A* **1970**, 1688.

[129] D. J. Spielvogel, W. M. Davis, S. L. Buchwald, *Organometallics* **2002**, *21*, 3833.

[130] S. Imajo, K. Nakanishi, M. Roberts, S. J. Lippard, T. Nozoe, *J. Am. Chem. Soc.* **1983**, *105*, 2071.

[131] W. M. Davis, M. M. Roberts, A. Zask, K. Nakanishi, T. Nozoe, S. J. Lippard, *J. Am. Chem. Soc.* **1985**, *107*, 3864.

[132] P. J. Chenier, A. S. Judd, T. L. Raguse, T. R. Hoye, *Tetrahedron Lett.* **1997**, *38*, 7341.

[133] K. Shindo, L.-C. Zhang, H. Wakabayashi, H. Miyamae, S. Ishikawa, T. Nozoe, *Heterocycles* **1995**, *40*, 913.

[134] W. Porzio, A. Musco, A. Immirzi, *Inorg. Chem.* **1980**, *19*, 2537.

[135] H. El-Amouri, A. A. Bahsoun, J. Fischer, J. A. Osborn, M.-T. Youinou, *Organometallics* **1991**, *10*, 3582.

[136] K. Burgess, W. A. van der Donk, S. A. Westcott, T. B. Marder, R. T. Baker, J. C. Calabrese, *J. Am. Chem. Soc.* **1992**, *114*, 9350.

[137] B. Longato, R. Coppo, G. Pilloni, C. Corvaja, A. Toffoletti, G. Bandoli, *J. Organomet. Chem.* **2001**, *637*, 710.

[138] N. Mezailles, P. Rosa, L. Ricard, F. Mathey, P. Le Floch, *Organometallics* **2000**, *19*, 2941.

[139] V. K. Sabirov, Y. T. Struchkov, A. S. Batsanov, M. A. Azizov, *Koord. Khim.* **1982**, *8*, 1623.

[140] D. W. Phelps, D. B. Losee, W. E. Haltfield, D. J. Hodgson, *Inorg. Chem.* **1976**, *15*, 3147.

[141] C. Zanchini, R. D. Willett, *Inorg. Chem.* **1990**, *29*, 3027.

[142] J. K. Garland, K. Emerson, M. R. Pressprich, *Acta Crystallogr. Sect. C* **1990**, *46*, 1603.

[143] R. L. Harlow, W. J. Wells III, G. W. Watt, S. H. Simonsen, *Inorg. Chem.* **1974**, *13*, 2106.

[144] G. S. Long, M. Wei, R. D. Willett, *Inorg. Chem.* **1997**, *36*, 3102.

[145] P. Guionneau, G. Bravic, J. Gaultier, D. Chasseau, M. Kurmoo, D. Kanazawa, P. Day, *Acta Crystallogr. Sect. C* **1994**, *50*, 1894.

[146] T. Mori, F. Sakai, G. Saito, H. Inokuchi, *Chem. Lett.* **1987**, 927.

[147] D. N. Anderson, R. D. Willett, *Inorg. Chim. Acta* **1974**, *8*, 167.

[148] R. D. Willett, F. H. Jardine, I. Rouse, R. J. Wong, C. P. Landee, M. Numata, *Phys. Rev. B* **1981**, *24*, 5372.

[149] L. P. Battaglia, A. B. Corradi, G. Marcotrigiano, L. Menabue, G. C. Pellacani, *Inorg. Chem.* **1982**, *21*, 3919.

[150] K. Dyrek, J. Goslar, S. A. Hodorowicz, S. K. Hoffmann, B. J. Oleksyn, A. Weselucha-Birczynska, *Inorg. Chem.* **1987**, *26*, 1481.

[151] L. Antolini, L. Menabue, G. C. Pellacani, M. Saladini, G. Marcotrigiano, W. Porzio, *J. Chem. Soc. Dalton Trans.* **1981**, 1753.

[152] W. K. Reagen, L. J. Radonovich, *J. Am. Chem. Soc.* **1989**, *111*, 3881.

[153] M. Haufe, R. D. Kohn, G. Kociok-Kohn, A. C. Filippou, *Inorg. Chem. Commun.* **1998**, *1*, 163.

[154] E. Balogh-Hergovich, J. Kaizer, G. Speier, G. Huttner, A. Jacobi, *Inorg. Chem.* **2000**, *39*, 4224.

[155] D.-M. Wang, B.-Y. Xue, R.-N. Yang, D.-M. Jin, L.-R. Chen, B.-S. Luo, *Jiegou Huaxue* **1997**, *16*, 287.

[156] H.-J. Drexler, H. Reinke, H.-J. Holdt, *Chem. Ber.* **1996**, *129*, 807.

[157] S. M. Carrier, C. E. Ruggiero, R. P. Houser, W. B. Tolman, *Inorg. Chem.* **1993**, *32*, 4889.

[158] T. Ogihara, S. Hikichi, M. Akita, Y. Moro-oka, *Inorg. Chem.* **1998**, *37*, 2614.

[159] K. Yoon, G. Parkin, *Polyhedron* **1995**, *14*, 811.

[160] J. A. Halfen, V. G. Young Jr., W. B. Tolman, *J. Am. Chem. Soc.* **1996**, *118*, 10920.

[161] H. Aneetha, Y.-H. Lai, S.-C. Li, K. Panneerselvam, T.-H. Lu, C.-S. Chung, *J. Chem. Soc. Dalton Trans.* **1999**, 2885.

[162] W. M. Davis, A. Zask, K. Nakanishi, S. J. Lippard, *Inorg. Chem.* **1985**, *24*, 3737.

[163] F. H. Allen, O. Kennard, *Chem. Des. Autom. News* **1993**, *8*, 31.

[164] *SHAPE*; M. Llunell, D. Casanova, J. Cirera, J. M. Bofill, P. Alemany, S. Alvarez, M. Pinsky, D. Avnir, version 1.1, Barcelona, **2003**.